Title: (U) A Theoretical Study of Asay Foil Trajectories

Author(s): Tregillis, Ian Lee

Intended for: Report

Issued: 2021-03-19

(U) A Theoretical Study of Asay Foil Trajectories

I. L. Tregillis, XCP-6

Abstract

We consider the trajectory of a generic Asay foil ejecta momentum diagnostic sensor, for scenarios where ejecta are produced at a planar surface and fly ballistically through a perfect vacuum to the sensor. To do so, we build upon a previously established mathematical formalism derived for the analytic study of stationary sensors (i.e., piezopins). First, we derive the momentum conservation equation for the problem, in a form amenable to accelerating sensors, in terms of a generic ejecta source areal mass function ("source model"). This defines an integro-differential equation (IDE) for the foil trajectory. When ejecta production is instantaneous—as is generally assumed in momentum diagnostic data analyses—the IDE can be cast in a highly compact form. This compact IDE leads to an *implicit* and easily calculable closed-form solution for the foil trajectory in a perfect system, as long as the ejecta particle velocity distribution is twice-integrable. General properties of the instant-production trajectory solution indicate the existence of a boundary condition the particle velocity distribution must satisfy in order for the analytically predicted foil trajectories to be compatible with certain features commonly observed in foil data. This boundary condition is identical to one derived previously from a consideration of piezopin data. Armed with the analytic solution for instant production, we also consider various techniques used to extract time-dependent cumulative ejecta masses from foil trajectories, and derive an expression for the error imposed by using an approximated equation of motion. This analytic trajectory solution furthermore makes it possible to examine the common practice of presenting inferred cumulative ejecta masses as a function of a normalized implied velocity; we derive conditions under which this methodology is and is not meaningful. We also propose a strategy for extending the instant-production trajectory solution to time-dependent source functions.

Contents

List of Figures

1 Statement of the Problem

This work is built upon a mathematical formalism originally developed for analytic examinations of piezoelectric ejecta measurements (i.e., for motionless sensors). That formalism—including its derivation, its application to problems of interest, and key results obtained from its use—has been extensively documented elsewhere [1–3]. Thus, for the sake of expedience, this work will cite previously derived results as necessary, referring the reader to the relevant documentation.

The problem of interest concerns the dynamical evolution of an ejecta cloud launched into vacuum from a singly shocked planar metal surface. In particular, we consider a situation where this cloud impinges upon a downstream sensor (an "Asay foil," or "foil" [4–6]) which subsequently undergoes acceleration owing to perfectly inelastic momentum transfer. Under certain circumstances, with the appropriate assumptions, measuring the time-dependent foil trajectory can yield information about the ejecta cloud, including the time-dependent accumulation of mass on the sensor.

For the purposes of this study, we consider a system that exactly embodies the assumptions built into the standard momentum-diagnostic analysis procedure. At the shock breakout time $t_0 = 0$ a planar free surface initially situated at $z = 0$ (these conventions simplify the derivations with no loss of generality) undergoes an instantaneous acceleration to constant lab-frame velocity u_{fs}. Ejecta production also begins at t_0. (The standard analysis procedure assumes this process is instantaneous, but here we relax that requirement, seeking solutions for sustained production, with instantaneous ejecta production as a special limiting case.) At some later time, t_c (for "time of creation"), an ejecta particle is launched from the free surface with relative velocity w and lab frame velocity $u = w + u_{fs}$. This flies ballistically through the perfect vacuum toward an Asay foil initially situated at distance z_{f0} from the unperturbed free surface. The foil is characterized by a clean areal mass μ_f. The particle collides perfectly inelastically with the foil at measurement time t. The foil accelerates as material accretes upon it, thus exhibiting a trajectory $z_f(t)$. In an experiment, the foil velocity $v_f(t) = \dot{z}_f(t)$ constitutes the physics measurement.

The ejecta particles are assumed to travel collinearly to the sensor with a long mean free path to scattering, so that neither the particle velocities nor the longitudinal ejecta cloud mass per unit area change in transit. The foil supports are disregarded in this treatment; an extensive examination of foil technologies has shown that for the purpose of analyzing the trajectory, well-designed foils can be justifiably approx-

imated as "free floating" objects [6]. Throughout, we assume the foil is sufficiently thin that corrections for thick-plate effects (e.g., time delays between particle impacts on the collection side and velocity changes on the probe side) can be disregarded [5].

The problem geometry is defined such that all quantities are nonnegative. The peak ejecta relative velocity is $\hat{w}$, and the peak ejecta lab-frame velocity (i.e., the velocity of the leading edge of the cloud) is $\hat{u} = \hat{w} + u_{fs}$. This setup is depicted in Fig. 1.

The problem: *Given a known source function $m_c(w, t_c)$, we seek a self-consistent analytic solution for the subsequent foil trajectory $z_f(t)$.*

Alternatively, a secondary but still interesting result would be to place nontrivial constraints on the functional form of m_c given a known $z_f(t)$. Approximate solutions for quasistatic foil motion are easy to derive, but as shown in §3.8.1 they have limited applicability.

A source areal mass function (AMF) [1,2] (m_c) is the mathematical representation of a physics hypothesis for ejecta production: a "source model." This AMF represents a distribution function for ejecta mass produced per unit area of the source, in particles of relative velocity (w) at a given creation instant (t_c). Thus it carries units of mass per unit volume (mass per unit area per velocity per time).

A closed-form solution for the foil trajectory would constitute a powerful tool for physics model validation, enabling quantitative "apples-to-apples" comparisons between ejecta source model predictions and Asay foil data. A similar approach applied to piezoelectric ejecta measurements has proven highly beneficial to both model validation and code verification efforts [1,3].

2
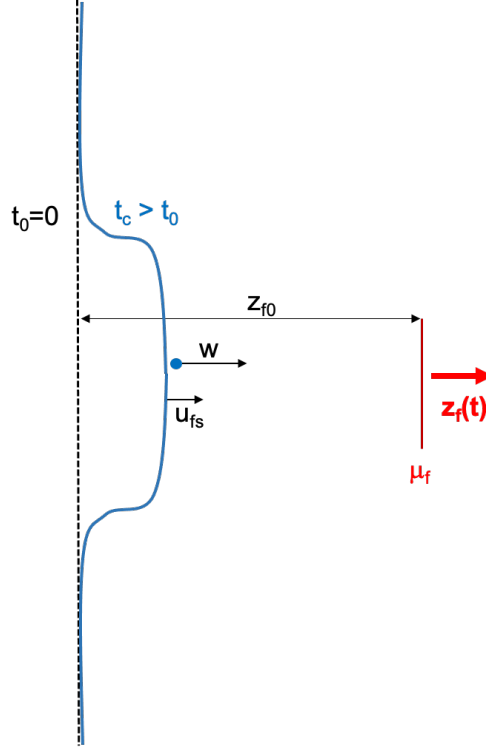
Figure 1: A free surface facing into vacuum is initially at rest in the lab frame (dashed black line). At $t_0 = 0$, that surface is shocked, liquefied, and instantaneously uniformly accelerated to constant lab-frame velocity u_{fs} (blue line). At creation time t_c, an ejecta particle is launched from the free surface with relative velocity w and lab-frame velocity $u = w + u_{fs}$. The source function $m_c(w, t_c)$ encodes the time-dependent distribution function for all such particles. The ejecta fly ballistically toward an Asay foil (red) initially at rest at distance z_{f0} from the unperturbed surface, and which has areal density μ_f. Particles begin to hit the foil (with perfectly inelastic collisions) at measurement time t_{a0}, at which point the foil undergoes a smooth continual acceleration with trajectory $z_f(t)$. The peak relative particle velocity is $\hat{w}$, which can be treated as time-independent for our purposes. Experimental data suggest the particle relative velocities extend down to $w = 0$, meaning there is no gap between the cloud and the free surface of liquefied metal. Data collection ends at some final measurement time t_{fs}, when the free surface slams into the sensor and destroys it. The sought-after solution is not required to handle the moment $t = t_{fs}$, but should work asymptotically close to t_{fs}.

3

2   Derivation of the Integro-Differential Equation

This problem effectively has three frames of reference: the lab frame (i.e., the frame of reference pinned to a stationary sensor, such as a piezoelectric pin); a frame co-moving with the post-shock free surface (ejecta source models are naturally specified in this frame); and a *noninertial* frame associated with the accelerating foil. For stationary sensors (pins), momentum transfer calculations are most naturally performed in the sensor (lab) frame. Here, working in the sensor frame is complicated by the presence of an *unknown* time-dependent transformation between that frame and the others. However, because the quantity of interest is the *lab frame* foil trajectory, sensor-frame calculations are unnecessary.

Consider a stationary sensor located at $z = h$. The time-dependent ejecta areal mass accumulation is given by [1, 2]

$$m\left(h;t\right) = \int_{\frac{h}{t}-u_{fs}}^{\hat{w}} \int_{t_0}^{t_c(h;w,t)} m_c\left(w,t_c\right) \, \mathrm{d}t_c \, \mathrm{d}w = \int_{\frac{h}{t}-u_{fs}}^{\hat{w}} \int_0^{\frac{\left(w+u_{fs}\right)t-h}{w}} m_c\left(w,t_c\right) \, \mathrm{d}t_c \, \mathrm{d}w$$

$$= \int_0^{\hat{w}} \int_0^{\frac{\left(w+u_{fs}\right)t-h}{w}} m_c\left(w,t_c\right) \, \mathrm{d}t_c \, \mathrm{d}w \,. \quad (2.1)$$

The lower limit on the velocity integration is defined by the causality condition: particles slower than this cannot arrive at the sensor by measurement time t. The function $t_c(h; w, t)$ is the time at which particles of relative velocity w must be created in order to arrive at $z = h$ at time t. Because this function is negative for velocities below the causality limit, and because the source function is identically zero for $t_c < t_0 = 0$ (because no particles are created prior to shock breakout), the lower limit on the velocity integration can be taken to 0 with no loss of generality.

Similarly, the total *lab frame* momentum deposited on the sensor (assuming perfectly inelastic collisions) is the *lab frame* momentum content of the accreted material:

$$p\left(h;t\right) = \int_0^{\hat{w}} \int_0^{\frac{\left(w+u_{fs}\right)t-h}{w}} m_c\left(w,t_c\right)\left(w + u_{fs}\right) \, \mathrm{d}t_c \, \mathrm{d}w \,. \quad (2.2)$$

4

How are these quantities correctly calculated on a moving sensor, $\mu_e(t)$ and $\pi_e(t)$?

Consider a foil initially located at $z_{f0} < h$, with an acceleration history such that $z_f\left(t < \tilde{t}\right) < h$, $z_f\left(\tilde{t}\right) = h$, $z_f\left(t > \tilde{t}\right) > h$. When $z_f(t) < h$, material accumulates on the closer foil more rapidly than it would on the more distant stationary sensor:

$$\mu_e\left(t < \tilde{t}\right) > m\left(h; t < \tilde{t}\right) \qquad \pi_e\left(t < \tilde{t}\right) > p\left(h; t < \tilde{t}\right).$$

Conversely, when $z_f(t) > h$ particles that would have arrived on the stationary sensor exactly at time t have not yet arrived, meaning the subsequent accumulation is slower than on the stationary sensor:

$$\mu_e\left(t > \tilde{t}\right) < m\left(h; t > \tilde{t}\right) \qquad \pi_e\left(t > \tilde{t}\right) < p\left(h; t > \tilde{t}\right).$$

Because the instantaneous accumulation on the sensor at time $\tilde{t}$ depends only on the particle velocities and the travel distance, $z_f\left(\tilde{t}\right) = h$, not the instantaneous foil velocity,

$$\mu_e\left(\tilde{t}\right) = m\left(h; \tilde{t}\right) \qquad \pi_e\left(\tilde{t}\right) = p\left(h; \tilde{t}\right).$$

In general, then,

$$\mu_e(t) = m\left[z_f(t); t\right] = \int_0^{\hat{w}} \int_0^{\frac{\left(w + u_{fs}\right)t - z_f(t)}{w}} m_c\left(w, t_c\right) \, \mathrm{d}t_c \, \mathrm{d}w \qquad (2.3)$$

$$\pi_e(t) = p\left[z_f(t); t\right] = \int_0^{\hat{w}} \int_0^{\frac{\left(w + u_{fs}\right)t - z_f(t)}{w}} m_c\left(w, t_c\right)\left(w + u_{fs}\right) \, \mathrm{d}t_c \, \mathrm{d}w. \qquad (2.4)$$

Momentum conservation requires

$$\left[\mu_f + \mu_e(t)\right] \dot{z}_f(t) = \pi_e(t) \qquad (2.5)$$

$$\mu_f \, \dot{z}_f(t) + \dot{z}_f(t) \int_0^{\hat{w}} \int_0^{\frac{\left(w + u_{fs}\right)t - z_f(t)}{w}} m_c\left(w, t_c\right) \, \mathrm{d}t_c \, \mathrm{d}w = \int_0^{\hat{w}} \int_0^{\frac{\left(w + u_{fs}\right)t - z_f(t)}{w}} m_c\left(w, t_c\right)\left(w + u_{fs}\right) \, \mathrm{d}t_c \, \mathrm{d}w$$

5

so the key relationship is encoded in this integro-differential equation (IDE):

$$\mu_f \dot{z}_f + (\dot{z}_f - u_{fs}) \int\limits_0^{\hat{w}} \int\limits_0^{\frac{(w+u_{fs})t-z_f}{w}} m_c(w, t_c) \, \mathrm{d}t_c \, \mathrm{d}w = \int\limits_0^{\hat{w}} \int\limits_0^{\frac{(w+u_{fs})t-z_f}{w}} w \, m_c(w, t_c) \, \mathrm{d}t_c \, \mathrm{d}w$$

(2.6)

The problem of interest is to solve this equation for $z_f(t)$, given $m_c(w, t_c)$.

As shown below, Eqn. 2.6 can be reduced to a far more compact form. Before continuing with that derivation, we first confirm that the IDE yields the correct result for a simple problem with a known solution.

2.1   Sanity Check: Single Particle

The simplest test problem represents a single particle launched from the source:

$$m_c(w, t_c) = m_0 \, \delta(w - \tilde{w}) \, \delta(t_c)$$

where m_0 and $\tilde{w}$ are positive constants and and δ denotes the Dirac delta function.

When applied to Eqn. 2.6, this form for the source function causes the integration over t_c to be nonzero long as $\frac{(w+u_{fs})t-z_f}{w} > 0$ for a given fixed measurement time (t), or equivalently when $w > \frac{z_f}{t} - u_{fs}$ (acknowledging a potentially subtle detail when the upper limit of integration is exactly zero). So for all instant production scenarios, the IDE simplifies to

$$\mu_f \dot{z}_f + m_0 (\dot{z}_f - u_{fs}) \int\limits_{\frac{z_f}{t}-u_{fs}}^{\hat{w}} f(w) \, \mathrm{d}w = m_0 \int\limits_{\frac{z_f}{t}-u_{fs}}^{\hat{w}} f(w) \, w \, \mathrm{d}w$$

and because $\hat{w}$ is the maximum physically allowable value for w, $f(w) \equiv 0$ for $w > \hat{w}$ and the upper limits of integration can be taken to infinity as necessary.

Now the w integrations are zero if $\frac{z_f}{t} - u_{fs} > \tilde{w}$, or equivalently when $t < \frac{z_f}{\tilde{w}+u_{fs}}$. The denominator is the lab-frame particle velocity, so this is simply the causality requirement: prior to particle arrival the sensor must remain motionless, and indeed we have $\mu_f \, \dot{z}_f = 0 \implies \dot{z}_f = 0$.

6

For any causal measurement time (after particle arrival), the velocity delta function is satisfied, yielding

$$\mu_f \dot{z}_f + m_0 \left(\dot{z}_f - u_{fs} \right) = m_0 \, \tilde{w}$$

or

$$\dot{z}_f = \frac{m_0}{\mu_f + m_0} \left(\tilde{w} + u_{fs} \right)$$

which is the correct answer to this trivial conservation of momentum problem.

2.2 Derivation of the Compact IDE

Here we derive the final, compact, form of the integro-differential equation.

We begin by defining the generalized ejecta velocity

$$\zeta(t) \equiv \frac{z_f(t)}{t - t_0} - u_{fs} = \frac{z_f(t)}{t} - u_{fs} \tag{2.7}$$

when $t_0 = 0$. As will become clear, this is the natural velocity coordinate for single-shock problems. Furthermore let $t_{a0} \equiv \frac{z_{f0}}{\hat{u}}$ be the time of first ejecta arrival on the foil, and let t_{fs} be the time at which the free surface arrives at the foil. The boundary conditions

$$\zeta \left(t_{a0} \right) = \frac{z_{f0}}{\frac{z_{f0}}{\hat{u}}} - u_{fs} = \hat{w} \tag{2.8}$$

$$\zeta \left(t_{fs} \right) = \frac{u_{fs} \, t_{fs}}{t_{fs}} - u_{fs} = 0 \tag{2.9}$$

immediately follow. Furthermore,

$$z_f = \left(\zeta + u_{fs} \right) t$$

$$v_f = \dot{z}_f = \dot{\zeta} \, t + \zeta + u_{fs} \tag{2.10}$$

$$\dot{v}_f = \ddot{\zeta} \, t + 2\dot{\zeta} \tag{2.11}$$

and because causality requires $v_f \left(t_{a0} \right) = 0$, we obtain the initial condition

$$\dot{\zeta} \left(t_{a0} \right) = -\frac{\hat{u}}{t_{a0}} = -\frac{\hat{u}^2}{z_{f0}} = -\frac{z_{f0}}{t_{a0}^2} \, . \tag{2.12}$$

Meanwhile,

$$\left(w + u_{fs} \right) t - z_f = \left(w + u_{fs} \right) t - \left(\zeta + u_{fs} \right) t = \left(w - \zeta \right) t$$

7

so when written in terms of ζ rather than z_f Eqn. 2.6 becomes

$$\mu_f \, u_{fs} + \left(\dot{\zeta} \, t + \zeta\right) \left[\mu_f + \int_0^{\hat{w}} \int_0^{\frac{(w-\zeta)t}{w}} m_c \left(w, t_c\right) \, \mathrm{d}t_c \, \mathrm{d}w\right] = \int_0^{\hat{w}} \int_0^{\frac{(w-\zeta)t}{w}} w \, m_c \left(w, t_c\right) \mathrm{d}t_c \, \mathrm{d}w \,.$$

(2.13)

Now note

$$\frac{\mathrm{d}}{\mathrm{d}t} \left[(w - \zeta) \, t\right] = w - \zeta - \dot{\zeta} \, t \implies \dot{\zeta} \, t + \zeta = w - \frac{\mathrm{d}}{\mathrm{d}t} \left[(w - \zeta) \, t\right] \,,$$

and because $\dot{\zeta} \, t + \zeta$ is not a function of w,

$$\left(\dot{\zeta} \, t + \zeta\right) \int_0^{\hat{w}} \int_0^{\frac{(w-\zeta)t}{w}} m_c \left(w, t_c\right) \, \mathrm{d}t_c \, \mathrm{d}w = \int_0^{\hat{w}} \left(\dot{\zeta} \, t + \zeta\right) \int_0^{\frac{(w-\zeta)t}{w}} m_c \left(w, t_c\right) \, \mathrm{d}t_c \, \mathrm{d}w$$

$$= \int_0^{\hat{w}} \left\{w - \frac{\mathrm{d}}{\mathrm{d}t} \left[(w - \zeta) \, t\right]\right\} \int_0^{\frac{(w-\zeta)t}{w}} m_c \left(w, t_c\right) \, \mathrm{d}t_c \, \mathrm{d}w$$

$$= \int_0^{\hat{w}} \int_0^{\frac{(w-\zeta)t}{w}} w \, m_c \left(w, t_c\right) \, \mathrm{d}t_c \, \mathrm{d}w - \int_0^{\hat{w}} \frac{\mathrm{d}}{\mathrm{d}t} \left[(w - \zeta) \, t\right] \int_0^{\frac{(w-\zeta)t}{w}} m_c \left(w, t_c\right) \, \mathrm{d}t_c \, \mathrm{d}w \,,$$

so substitution into Eqn. 2.13 yields

$$\mu_f \, u_{fs} + \mu_f \left(\dot{\zeta} \, t + \zeta\right) - \int_0^{\hat{w}} \frac{\mathrm{d}}{\mathrm{d}t} \left[(w - \zeta) \, t\right] \int_0^{\frac{(w-\zeta)t}{w}} m_c \left(w, t_c\right) \, \mathrm{d}t_c \, \mathrm{d}w = 0$$

or

$$\mu_f \left(\zeta + u_{fs}\right) t - \int_0^{\hat{w}} \left[(w - \zeta) \, t\right] \int_0^{\frac{(w-\zeta)t}{w}} m_c \left(w, t_c\right) \, \mathrm{d}t_c \, \mathrm{d}w = \kappa$$

(2.14)

where κ is a constant of integration. The domain of the problem guarantees $t \geq$

8

$t_{a0} > 0$, so

$$\mu_f \left(\zeta + u_{fs}\right) - \int_0^{\hat{w}} (w - \zeta) \int_0^{\frac{(w-\zeta)t}{w}} m_c\left(w, t_c\right) \mathrm{d}t_c \, \mathrm{d}w = \frac{\kappa}{t}$$

$$\mu_f \left(\zeta + u_{fs}\right) + \zeta \int_0^{\hat{w}} \int_0^{\frac{(w-\zeta)t}{w}} m_c\left(w, t_c\right) \mathrm{d}t_c \, \mathrm{d}w - \int_0^{\hat{w}} \int_0^{\frac{(w-\zeta)t}{w}} w \, m_c\left(w, t_c\right) \mathrm{d}t_c \, \mathrm{d}w = \frac{\kappa}{t} \, .$$

Using Eqn. 2.13 to substitute the third term on the left side yields

$$\mu_f \left(\zeta + u_{fs}\right) + \zeta \int_0^{\hat{w}} \int_0^{\frac{(w-\zeta)t}{w}} m_c\left(w, t_c\right) \mathrm{d}t_c \, \mathrm{d}w$$

$$- \left\{ \mu_f \, u_{fs} + \left(\dot{\zeta} t + \zeta\right) \left[\mu_f + \int_0^{\hat{w}} \int_0^{\frac{(w-\zeta)t}{w}} m_c\left(w, t_c\right) \mathrm{d}t_c \, \mathrm{d}w \right] \right\} = \frac{\kappa}{t}$$

or

$$-\mu_f \dot{\zeta} t - \dot{\zeta} t \int_0^{\hat{w}} \int_0^{\frac{(w-\zeta)t}{w}} m_c\left(w, t_c\right) \mathrm{d}t_c \, \mathrm{d}w = \frac{\kappa}{t}$$

$$\dot{\zeta} \left[\mu_f + \int_0^{\hat{w}} \int_0^{\frac{(w-\zeta)t}{w}} m_c\left(w, t_c\right) \mathrm{d}t_c \, \mathrm{d}w \right] = -\frac{\kappa}{t^2} \, . \tag{2.15}$$

The integral term is exactly $m_t \left[z_f(t); t\right]$, the true cumulative ejecta areal mass on the sensor at time t. At the instant of first arrival at the sensor, t_{a0}, Eqn. 2.15 becomes

$$\mu_f \dot{\zeta}\left(t_{a0}\right) = -\frac{\kappa}{t_{a0}^2} \, .$$

If the sensor is initially motionless, the initial condition $\dot{\zeta}\left(t_{a0}\right) = -\frac{\hat{u}}{t_{a0}}$ fixes the integration constant to $\kappa = \mu_f \, \hat{u} \, t_{a0} = \mu_f \, z_{f0}$ so the original IDE (Eqn. 2.6) can be reduced to the compact form

$$\boxed{\dot{\zeta} \left[\mu_f + \int_0^{\hat{w}} \int_0^{\frac{(w-\zeta)t}{w}} m_c\left(w, t_c\right) \mathrm{d}t_c \, \mathrm{d}w \right] = -\frac{\mu_f \, z_{f0}}{t^2} \, .} \tag{2.16}$$

To reiterate, then, the problem of interest is to solve Eqn. 2.16 for $\zeta(t)$, and therefore $z_f(t)$, given a known source function $m_c(w, t_c)$.

For future reference, in cases where the foil has $v_{f0} \equiv v_f(t_{a0}) \neq 0$ when ejecta begins to accrete upon it, the relation $\dot{\zeta}(t_{a0}) = v_f(t_{a0}) - \zeta(t_{a0}) - u_{fs}$ yields $\kappa = \mu_f(z_{f0} - t_{a0}v_{f0})$. The "affine" compact IDE for $t_0 \neq 0$ is given in §4.1.

3 General Implicit Solution for Instant Creation

A general implicit solution exists for instant-creation source functions,

$$m_c(w, t_c) = m_0 f(w) \delta(t_c) \tag{3.1}$$

where m_0 is a positive constant and $f(w)$ is the instantly-created particle velocity distribution. Mass conservation imposes a normalization requirement $\int_0^{\hat{w}} f(w)\, dw = \int_0^\infty f(w)\, dw = 1$ so m_0 is the total sourced ejecta areal mass in these problems.

We assume the velocity distribution is twice-integrable, and define [1]

$$F_1'(w) \equiv f(w)$$
$$F_2'(w) \equiv F_1(w)$$
$$F_2''(w) \equiv F_1'(w) \equiv f(w)$$

(This step is justified by the expectation that a real-world physics problem will disallow mathematically pathological velocity distributions.) Placing the instant-creation AMF into the compact IDE (Eqn. 2.16) yields

$$\frac{\mu_f}{m_0}\dot{\zeta} + \dot{\zeta} \int_\zeta^{\hat{w}} f(w)\, dw = -\frac{\mu_f}{m_0} \frac{z_{f0}}{t^2}$$

$$\frac{\mu_f}{m_0}\dot{\zeta} + \dot{\zeta} F_1(\hat{w}) - \dot{\zeta} F_1(\zeta) = -\frac{\mu_f}{m_0}\frac{z_{f0}}{t^2}$$

$$\left[\frac{\mu_f}{m_0} + F_1(\hat{w})\right]\dot{\zeta} - \frac{d}{dt}F_2(\zeta) = z_{f0}\frac{\mu_f}{m_0}\frac{d}{dt}\left(\frac{1}{t}\right)$$

$$\left[\frac{\mu_f}{m_0} + F_1(\hat{w})\right]\zeta - F_2(\zeta) = \frac{\mu_f}{m_0}\frac{z_{f0}}{t} - \nu$$

---

[1] The $F_{1,2}$ notation used here should not be confused with the hypergeometric function $_2F_1$.

where ν is an integration constant. Defining the (known) constants

$$\sigma \equiv \frac{\mu_f}{m_0} + F_1\left(\hat{w}\right) \qquad \lambda = z_{f0}\frac{\mu_f}{m_0}.$$

makes this

$$\sigma\,\zeta - F_2\left(\zeta\right) = \frac{\lambda}{t} - \nu\,.$$

When $t = t_{a0}$, this becomes

$$\left[\frac{\mu_f}{m_0} + F_1\left(\hat{w}\right)\right]\hat{w} - F_2\left(\hat{w}\right) = \frac{\mu_f}{m_0}\,\hat{u} - \nu$$

$$\implies \nu = \frac{\mu_f}{m_0}\,u_{fs} + F_2\left(\hat{w}\right) - \hat{w}\,F_1\left(\hat{w}\right)\,.$$

The implicit equation linking the measurement time t and ζ is therefore

$$\boxed{t = \frac{\lambda}{\sigma\,\zeta - F_2\left[\zeta\right] + \nu}} \tag{3.2}$$

where

$$\sigma = \frac{\mu_f}{m_0} + F_1\left(\hat{w}\right) \tag{3.3}$$

$$\lambda = z_{f0}\left(\frac{\mu_f}{m_0}\right) \tag{3.4}$$

$$\nu = \left(\frac{\mu_f}{m_0}\right)u_{fs} + F_2\left(\hat{w}\right) - \hat{w}\,F_1\left(\hat{w}\right) \tag{3.5}$$

$$F_2''(w) = F_1'(w) = f(w) \tag{3.6}$$

$$\zeta(t) = \frac{z_f(t)}{t} - u_{fs}\,.$$

(By construction, integration constants can be disregarded when deriving $F_{1,2}$ from a *smooth* distribution f. But if f is piecewise continuous, $F_{1,2}$ may contain additional integration constants in order to maintain continuity.) This implicit solution for ζ, and hence z_f, can be computed straightforwardly as $t\left(\zeta\right)$. Depending on the functional form of the particle velocity distribution, $f(w)$, this implicit solution may be invertible to the form $\zeta(t)$. As shown below, this is not possible in all cases. When the inversion is not possible, the implicit solution is still sufficient for computing trajectories with arbitrary accuracy, as for instance a Python calculation will involve computing arrays of ζ and t values anyway.

The implicit solution has several interesting properties. Chief among them is the direct calculation of the free surface arrival time at the accelerated sensor, t_{fs}. From the boundary condition $\zeta(t_{fs}) = 0$ we get

$$t_{fs} = \frac{\lambda}{\nu - F_2(0)} = \frac{z_{f0}\left(\frac{\mu_f}{m_0}\right)}{\left(\frac{\mu_f}{m_0}\right)u_{fs} + F_2(\hat{w}) - F_2(0) - \hat{w} F_1(\hat{w})}$$

$$= \frac{z_{f0}\left(\frac{\mu_f}{m_0}\right)}{\left(\frac{\mu_f}{m_0}\right)u_{fs} - \int_0^{\hat{w}} w f(w)\,\mathrm{d}w} = \frac{z_{f0}\left(\frac{\mu_f}{m_0}\right)}{\left(\frac{\mu_f}{m_0}\right)u_{fs} - \langle w \rangle} = \frac{z_{f0}}{u_{fs} - \frac{m_0}{\mu_f}\langle w \rangle}$$

where $\langle w \rangle$ denotes the mean velocity in the distribution:

$$\langle w \rangle = \frac{\int_0^{\infty} w f(w)\,\mathrm{d}w}{\int_0^{\infty} f(w)\,\mathrm{d}w} = \frac{\int_0^{\hat{w}} w f(w)\,\mathrm{d}w}{\int_0^{\hat{w}} f(w)\,\mathrm{d}w} = \int_0^{\hat{w}} w f(w)\,\mathrm{d}w .$$

When $u_{fs} < \frac{m_0}{\mu_f}\langle w \rangle$, then $t_{fs} < 0$, which is unphysical (acausal). Thus the free surface will never catch the accelerated foil if $\langle w \rangle > \frac{\mu_f}{m_0} u_{fs}$. When these quantities are equal, $t_{fs} \to \infty$ and the free surface will just catch the foil at infinity. For physically realizable systems, causality also requires $t_{fs} > t_{a0}$, or

$$\frac{z_{f0}}{u_{fs} - \frac{m_0}{\mu_f}\langle w \rangle} > \frac{z_{f0}}{\hat{u}} \implies \hat{u} > u_{fs} - \frac{m_0}{\mu_f}\langle w \rangle \implies \hat{w} > -\frac{m_0}{\mu_f}\langle w \rangle$$

so this condition is always satisfied.

3.1 Example: Instant Boxcar Distribution

Consider a constant uniform velocity distribution. Normalization makes this $f(w) = \hat{w}^{-1}$, so

$$F_1(w) = \frac{w}{\hat{w}} \qquad F_2(w) = \frac{w^2}{2\hat{w}}$$

which lead to

$$\sigma = 1 + \frac{\mu_f}{m_0}$$

$$\nu = \left(\frac{\mu_f}{m_0}\right)u_{fs} - \frac{\hat{w}}{2}$$

12

and a simple quadratic for ζ:

$$-\frac{\zeta^2}{2\hat{w}} + \left(1 + \frac{\mu_f}{m_0}\right)\zeta - \left[\frac{\hat{w}}{2} - \left(\frac{\mu_f}{m_0}\right)u_{fs}\right] = \frac{z_{f0}}{t}\left(\frac{\mu_f}{m_0}\right).$$

The quadratic equation offers two solutions but the boundary condition $\zeta\left(t_{a0}\right) = \hat{w}$ requires the negative branch. With a little algebra, the solution can be written

$$\zeta(t) = \left[\left(1 + \frac{\mu_f}{m_0}\right) - \sqrt{\left(\frac{\mu_f}{m_0}\right)^2 + 2\frac{z_{f0}}{\hat{w}}\left(\frac{\mu_f}{m_0}\right)\left(\frac{1}{t_{a0}} - \frac{1}{t}\right)}\right]\hat{w}$$

and finally $z_f(t) = [\zeta(t) + u_{fs}]\,t$.

The free surface arrival time is simply

$$t_{fs} = \frac{\lambda}{\nu - F_2(0)} = \frac{\lambda}{\nu} = \frac{z_{f0}}{u_{fs} - \frac{m_0}{\mu_f}\frac{\hat{w}}{2}}.$$

The result for typical parameter values found in the literature [7] is plotted in Figure 2. The trajectory z_f is plausible, and qualitatively in line with expectations based on physical intuition and explorations based on rough numerical integrations. (The abrupt acceleration of the foil, $\dot{v}_f\left(t_{a0}\right) > 0$, might be at odds with what is seen experimentally, but that is not surprising as we know the boxcar velocity distribution is not generated in such experiments.)
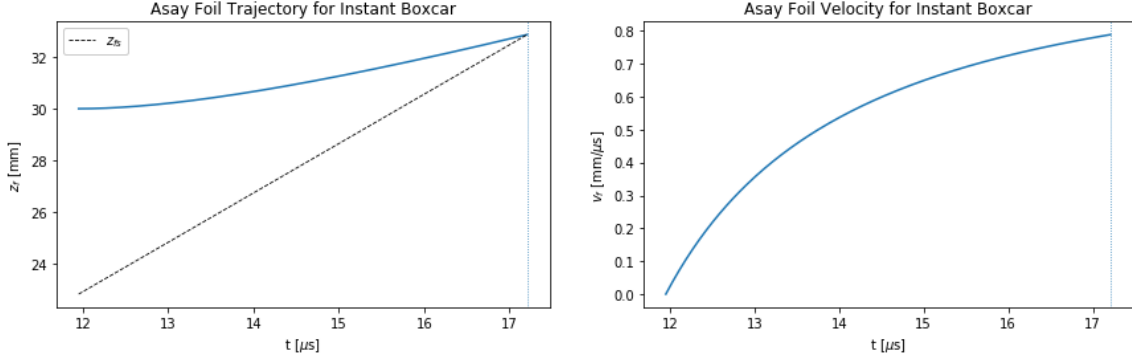
Figure 2: The analytic solution for an instantly created boxcar velocity distribution, computed using a set of parameter values typical of ejecta experiments found in the literature. Here the titanium Asay foil is 100 μm thick ($\mu_f = 45.06$ mg/cm^2), $m_0 = 25$ mg/cm^2, $u_{fs} = 1.91$ mm/μs, $\hat{w} = 0.6$ mm/μs, and $z_{f0} = 30$ mm. Left: Asay foil trajectory, $z_f(t)$, co-plotted with the free surface location, $z_{fs}(t)$ (black). Right: Asay foil velocity, $\dot{z}_f(t) \equiv v_f(t)$.

13

3.2 Example: Instant Exponential Distribution

The exponential distribution has

$$f(w) = \kappa\,\mathrm{e}^{-\alpha\frac{w}{\hat{w}}} \qquad F_1(w) = -\frac{\kappa\hat{w}}{\alpha}\,\mathrm{e}^{-\alpha\frac{w}{\hat{w}}} \qquad F_2(w) = \frac{\kappa\hat{w}^2}{\alpha^2}\,\mathrm{e}^{-\alpha\frac{w}{\hat{w}}}$$

with $\alpha > 0$, which leads to

$$\sigma = \frac{\mu_f}{m_0} - \frac{\kappa\hat{w}}{\alpha}\,\mathrm{e}^{-\alpha}$$

$$\nu = \left(\frac{\mu_f}{m_0}\right)u_{fs} + \frac{\kappa\hat{w}}{\alpha^2}\,(1+\alpha)\,\mathrm{e}^{-\alpha}$$

and the implicit solution

$$-\frac{\kappa\hat{w}^2}{\alpha^2}\,\mathrm{e}^{-\alpha\frac{\zeta}{\hat{w}}} + \left[\frac{\mu_f}{m_0} - \frac{\kappa\hat{w}}{\alpha}\,\mathrm{e}^{-\alpha}\right]\zeta + \left[\frac{\kappa\hat{w}}{\alpha^2}\,(1+\alpha)\,\mathrm{e}^{-\alpha} + \left(\frac{\mu_f}{m_0}\right)u_{fs}\right] = \frac{z_{f0}}{t}\left(\frac{\mu_f}{m_0}\right).$$

Now let $y(t) \equiv \frac{\alpha}{\hat{w}}\,\zeta(t)$; the boundary conditions $y(t_{a0}) = \alpha$ and $y(t_{fs}) = 0$ follow. The result is an equation of the form

$$A\,\mathrm{e}^{-y(t)} + B\,y(t) - C = f(t)$$

where

$$A \equiv \frac{\kappa\,\hat{w}^2}{\alpha^2}$$

$$B \equiv \frac{\kappa\,\hat{w}^2}{\alpha^2}\,\mathrm{e}^{-\alpha} - \frac{\hat{w}}{\alpha}\frac{\mu_f}{m_0}$$

$$C \equiv \left[\left(\frac{\mu_f}{m_0}\right)u_{fs} + \frac{\kappa\,\hat{w}^2}{\alpha^2}\,(1+\alpha)\,\mathrm{e}^{-\alpha}\right]$$

$$f(t) \equiv -\frac{z_{f0}}{t}\left(\frac{\mu_f}{m_0}\right).$$

Then

$$y = \frac{f(t)+C}{B} - \frac{A}{B}\,\mathrm{e}^{-y} \equiv \kappa_0 + \kappa_1\,\mathrm{e}^{-y} \implies (y-\kappa_0)\,\mathrm{e}^{(y-\kappa_0)} = \kappa_1\,\mathrm{e}^{-\kappa_0}$$

so

$$y(t) = \kappa_0 + W\left(\kappa_1\,\mathrm{e}^{-\kappa_0}\right) = \frac{f(t)+C}{B} + W\left[-\frac{A}{B}\,\mathrm{e}^{-\frac{f(t)+C}{B}}\right]$$

14

where W is the Lambert W function. The solution requires the principle branch, W_0, when the argument is negative, and W_{-1} branch when the argument is positive.

The free surface arrival time is

$$t_{fs} = \frac{\lambda}{\nu - F_2(0)} = \frac{z_{f0}\left(\frac{\mu_f}{m_0}\right)}{\left(\frac{\mu_f}{m_0}\right)u_{fs} + \frac{\kappa\hat{w}}{\alpha^2}(1+\alpha)\,\mathrm{e}^{-\alpha} - \frac{\kappa\hat{w}^2}{\alpha^2}\,\mathrm{e}^{-\alpha}}.$$

Example results for $\alpha = 1$ & 7.2 are plotted in Fig. 3.
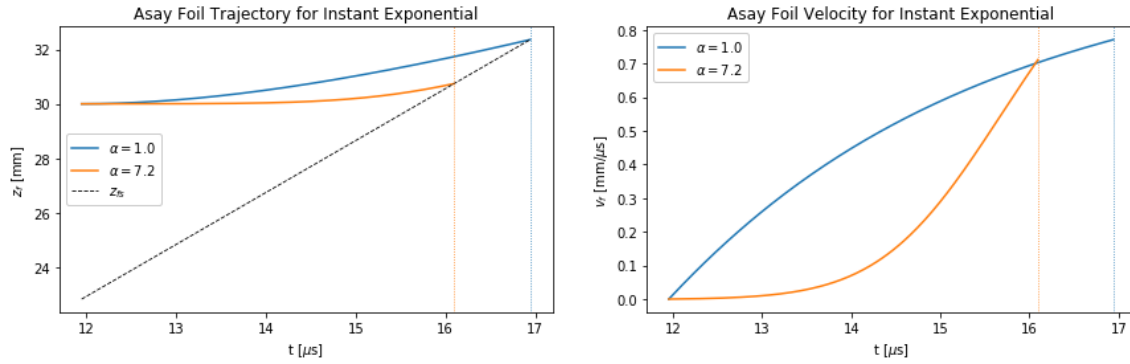
Figure 3: The analytic solution for an instantly created exponential velocity distribution computed for $\alpha = 1$ and $\alpha = 7.2$, using parameter values as in the boxcar example. Left: Asay foil trajectories, $z_f(t)$, co-plotted with the free surface location, $z_{fs}(t)$ (black). Right: Asay foil velocities, $\dot{z}_f(t) \equiv v_f(t)$.

Again, the z_f trajectories are plausible and in line with physical expectations. Interestingly, the $\alpha = 1$ solution exhibits a "convex" foil acceleration with $\dot{v}_f(t_{a0}) > 0$, while $\alpha = 7.2$ exhibits a "concave" foil acceleration, $\dot{v}_f(t_{a0}) \approx 0$. The latter is more consistent with physical expectations based on complementary data.

3.3 Example: Instant Power-Law Distribution

Consider an instantly created power-law velocity distribution

$$f(w) = \kappa \left(\frac{w + w_0}{\hat{w}}\right)^{-\alpha}$$

15

where as usual κ is the appropriate normalization constant, the positive constant w_0 is required to keep $f(w)$ finite at $w = 0$, and for convenience we require $0 < \alpha < 1$. Then

$$F_1(w) = \frac{\kappa \, \hat{w}^\alpha}{1 - \alpha} \, (w + w_0)^{1-\alpha} \qquad F_2(w) = \frac{\kappa \, \hat{w}^\alpha}{(1 - \alpha)\,(2 - \alpha)} \, (w + w_0)^{2-\alpha}$$

and

$$\sigma = \frac{\mu_f}{m_0} + \frac{\kappa \hat{w}^\alpha}{1 - \alpha} \, (w + w_0)^{1-\alpha}$$

$$\nu = \frac{\mu_f}{m_0} \, u_{fs} + \frac{\kappa \, \hat{w}^\alpha}{(1 - \alpha)\,(2 - \alpha)} \cdot (\hat{w} + w_0)^{2-\alpha} - \frac{\kappa \, \hat{w}^{1+\alpha}}{1 - \alpha} \cdot (\hat{w} + w_0)^{1-\alpha} \; .$$

In this case, the implicit equation is

$$\left(\frac{\mu_f}{m_0} + \frac{\kappa \hat{w}^\alpha}{1 - \alpha} \, (w + w_0)^{1-\alpha} \right) \zeta(t) - \frac{\kappa \, \hat{w}^\alpha}{(1 - \alpha)\,(2 - \alpha)} \, [\zeta(t) + w_0]^{2-\alpha}$$

$$+ \left[\frac{\mu_f}{m_0} \, u_{fs} + \frac{\kappa \, \hat{w}^\alpha}{(1 - \alpha)\,(2 - \alpha)} \cdot (\hat{w} + w_0)^{2-\alpha} - \frac{\kappa \, \hat{w}^{1+\alpha}}{1 - \alpha} \cdot (\hat{w} + w_0)^{1-\alpha} \right] = \frac{z_{f0}}{t} \frac{\mu_f}{m_0}$$

or

$$\left(\frac{\mu_f}{m_0} + \frac{\kappa \hat{w}^\alpha}{1 - \alpha} \, (w + w_0)^{1-\alpha} \right) \zeta(t) - \frac{\kappa \, \hat{w}^\alpha}{(1 - \alpha)\,(2 - \alpha)} \, [\zeta(t) + w_0]^{2-\alpha}$$

$$+ \left[\frac{\mu_f}{m_0} \, u_{fs} + \frac{\kappa \, \hat{w}^\alpha}{(1 - \alpha)\,(2 - \alpha)} \cdot (\hat{w} + w_0)^{2-\alpha} - \frac{\kappa \, \hat{w}^{1+\alpha}}{1 - \alpha} \cdot (\hat{w} + w_0)^{1-\alpha} - \frac{z_{f0}}{t} \frac{\mu_f}{m_0} \right] = 0 \, .$$

Unlike the quadratic polynomial obtained from the boxcar distribution, there is no general solution for the roots of this polynomial for any arbitrary value of α. In this case, a better approach is to work with the implicit solution $t\,(\zeta)$.

Example results for $w_0 = \hat{w}$ and $\alpha = 0.25,\ 0.50,\ \&\ 0.75$ are plotted in Fig. 4.

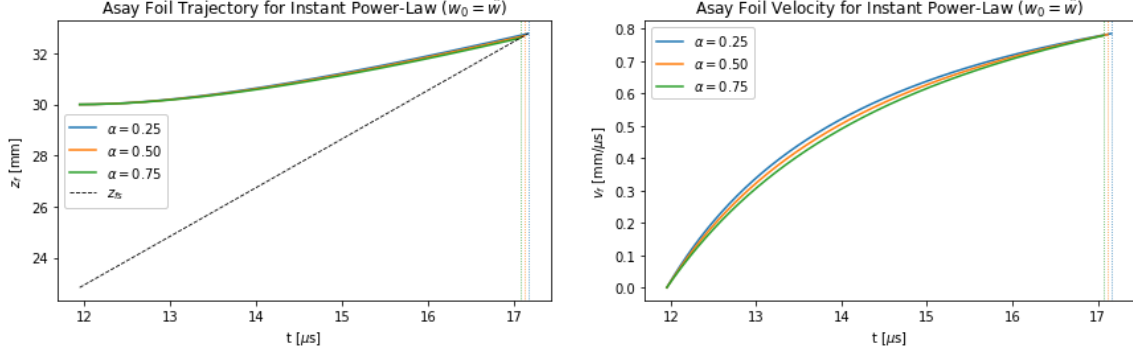**Figure 4:** The analytic solution for an instantly created power-law velocity distribution computed for $w_0 = \hat{w}$ and $\alpha = 0.25,\ 0.50,\ \&\ 0.75$, using parameter values as in the previous examples. Left: Asay foil trajectories, $z_f(t)$, co-plotted with the free surface location, $z_{fs}(t)$ (black). Right: Asay foil velocities, $\dot{z}_f(t) \equiv v_f(t)$.

3.4   Example: Instant SSVD

The self-similar velocity distribution (SSVD) [8,9] has the form

$$f(w) = \kappa_1 \, \mathrm{e}^{-\xi\frac{w}{\hat{w}}} + \kappa_2 \,.$$

This general form holds for both the original and modified (aka "dropped" or "boundary aware") [3] versions of the SSVD; in the latter case, $f\left(\hat{w}\right) \equiv 0$. Both versions of the SSVD adhere to the usual normalization requirement.

This leads to

$$F_1(w) = \kappa_2 \, w - \kappa_1 \left(\frac{\hat{w}}{\xi}\right) \mathrm{e}^{-\xi\frac{w}{\hat{w}}} \qquad F_2(w) = \kappa_2 \, \frac{w^2}{2} + \kappa_1 \left(\frac{\hat{w}}{\xi}\right)^2 \mathrm{e}^{-\xi\frac{w}{\hat{w}}}$$

and

$$\sigma = \frac{\mu_f}{m_0} + \kappa_2 \, \hat{w} - \kappa_1 \left(\frac{\hat{w}}{\xi}\right) \mathrm{e}^{-\xi}$$

$$\nu = \left(\frac{\mu_f}{m_0}\right) u_{fs} + \kappa_2 \, \frac{\hat{w}^2}{2} + \kappa_1 \left(\frac{\hat{w}}{\xi}\right)^2 \mathrm{e}^{-\xi} + \kappa_1 \left(\frac{\hat{w}^2}{\xi}\right) \mathrm{e}^{-\xi} - \kappa_2 \, \hat{w}^2$$

$$= \left(\frac{\mu_f}{m_0}\right) u_{fs} + \kappa_1 \, \hat{w}^2 \, \mathrm{e}^{-\xi} \left(\frac{1}{\xi} + \frac{1}{\xi^2}\right) - \kappa_2 \, \frac{\hat{w}^2}{2} \,.$$

17

For completeness, the resulting solution for $t(\zeta)$ is

$$t = \frac{z_{f0} \left(\frac{\mu_f}{m_0} \right)}{\left[\frac{\mu_f}{m_0} + \kappa_2 \hat{w} - \kappa_1 \left(\frac{\hat{w}}{\xi} \right) e^{-\xi} \right] \zeta - \kappa_2 \frac{\zeta^2}{2} - \kappa_1 \left(\frac{\hat{w}}{\xi} \right)^2 e^{-\xi \frac{\zeta}{\hat{w}}} + \left(\frac{\mu_f}{m_0} \right) u_{fs} + \kappa_1 \hat{w}^2 e^{-\xi} \left(\frac{1}{\xi} + \frac{1}{\xi^2} \right) - \kappa_2 \frac{\hat{w}^2}{2}}.$$

This is not invertible to a $\zeta(t)$ form, so the trajectory must be computed implicitly.

Example results for $\xi = 7.2$ are plotted in Fig. 5.
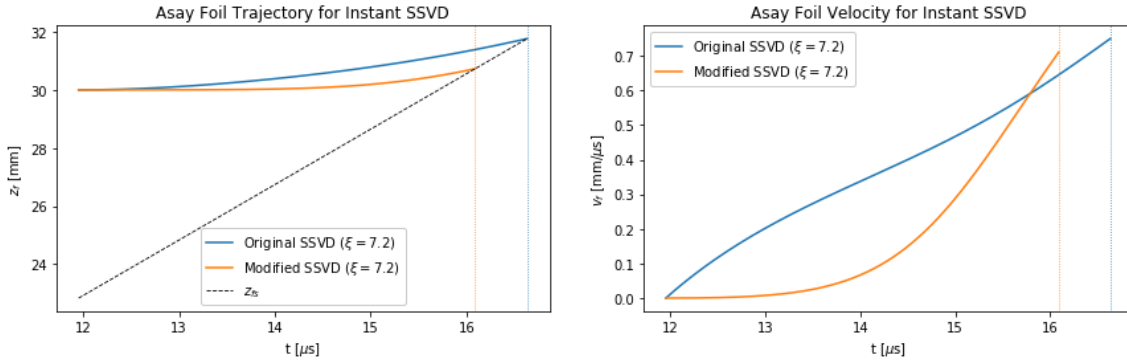
Figure 5: The analytic solution for an instantly created self-similar velocity distribution (SSVD) computed for $\xi = 7.2$, using parameter values as in the previous examples. Results for both the original and modified ("boundary aware") SSVD are shown. Left: Asay foil trajectories, $z_f(t)$, co-plotted with the free surface location, $z_{fs}(t)$ (black). Right: Asay foil velocities, $\dot{z}_f(t) \equiv v_f(t)$.

Notice that while the foil motion is similarly small for both cases, the original and modified SSVD solutions are distinguished by the time-dependence of the foil velocity. The original SSVD predicts a convex v_f, while the modified SSVD predicts a smoother start with a concave v_f.

3.4.1 Additional SSVD Variants: Linear and Exponential Tails

Two additional variations on the original SSVD are sometimes used in numerical simulations. These variants are designed to approximately satisfy boundary condition requirements obtained from a consideration of global properties of piezoelectric sensor data [3].

18

Both variants follow the original SSVD prescription up to a "cusp" velocity, w_c, with $0 < w_c < \hat{w}$. (The cusp velocity is a free parameter.) Above the cusp, the "linear tail" (LT) variant goes linearly to $f(\hat{w}) = 0$ with the generic form

$$f(w) = \begin{cases} \kappa_1 \, e^{-\xi \frac{w}{\hat{w}}} + \kappa_2 & 0 \le w \le w_c \\ \kappa_3 \, (w - w_c) + \kappa_4 & w_c < w \le \hat{w} \end{cases}$$

whereas the "exponential tail" (ET) variant drops exponentially to $f(\hat{w}) \approx 0$ via

$$f(w) = \begin{cases} \kappa_1 \, e^{-\xi \frac{w}{\hat{w}}} + \kappa_2 & 0 \le w \le w_c \\ \kappa_3 \, e^{-\alpha \frac{w}{\hat{w}}} & w_c < w \le \hat{w} \end{cases}$$

where here $\alpha > 0$ is also a free parameter.

Additional integration constants enter the problem when deriving *continuous* functions $F_{1,2}$ from these piecewise continuous velocity distributions. The mathematical derivations are straightforward and similar to those found in the preceding examples. Example results for $\xi = 7.2$, $w_c = 0.40$, and $\alpha = 10$ are plotted in Fig. 6.
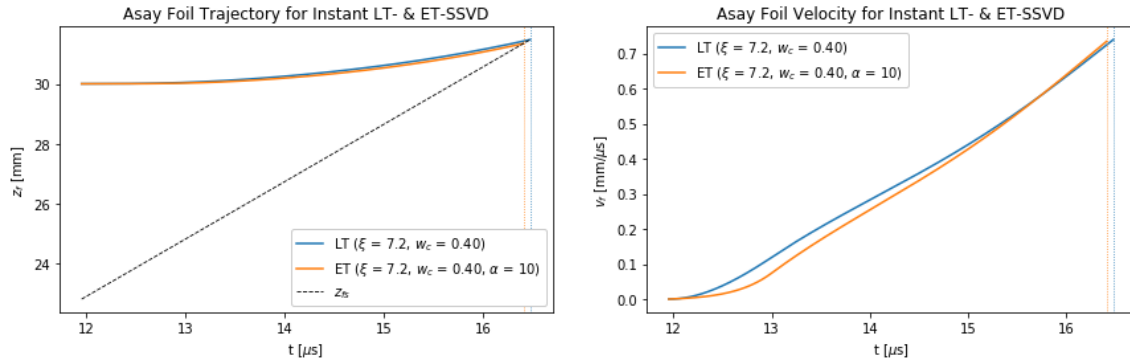
Figure 6: Analytic solutions for instantly created linear- (LT) and exponential-tail (ET) SSVD variants. These example calculations used $\xi = 7.2$ and $w_c = 0.40$, with an additional parameter $\alpha = 10$ in the ET variant. All other parameter values were set as in the previous examples. Left: Asay foil trajectories, $z_f(t)$, co-plotted with the free surface location, $z_{fs}(t)$ (black). Right: Asay foil velocities, $\dot{z}_f(t) \equiv v_f(t)$.

3.5 Combined Results

For direct comparison, the results from the preceding calculations for various instantly produced velocity distributions are co-plotted in Fig. 7. The distinction between smooth-start (concave) and hard-start (convex) velocity histories is clear.

19
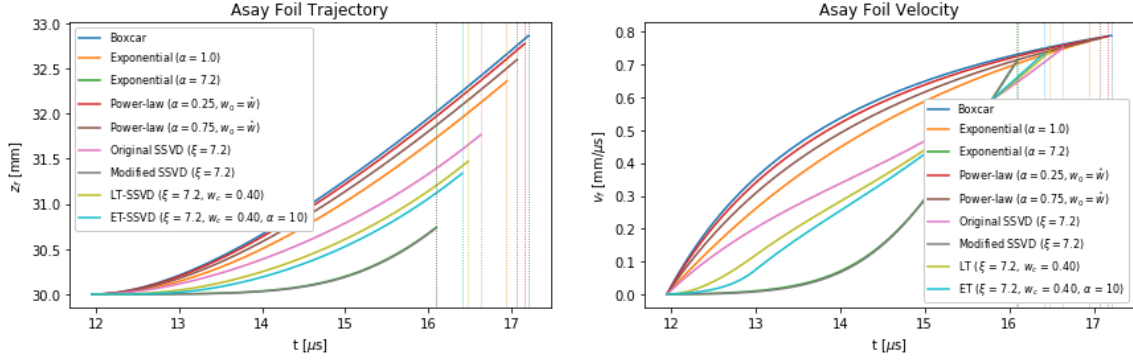
Figure 7: Combined results for instantly created boxcar, exponential, power-law, and self-similar (original and modified) velocity distributions. Left: Asay foil trajectories, $z_f(t)$. Right: Asay foil velocities, $\dot{z}_f(t) \equiv v_f(t)$. The vertical lines mark the analytically computed t_{fs} values.

3.6 Boundary Conditions for Instant-Production Scenarios

From the implicit solution,

$$\sigma\,\zeta - F_2\left(\zeta\right) + \nu = \frac{\lambda}{t}$$

$$\sigma\,\dot{\zeta} - \dot{\zeta}\,F_2'\left(\zeta\right) = -\frac{\lambda}{t^2}$$

$$\sigma\,\ddot{\zeta} - \ddot{\zeta}\,F_2'\left(\zeta\right) - \dot{\zeta}^2 F_2''\left(\zeta\right) = \frac{2\lambda}{t^3}$$

$$\ddot{\zeta}\left[\sigma - F_2'\left(\zeta\right)\right] - \dot{\zeta}^2 F_2''\left(\zeta\right) = \frac{2\lambda}{t^3}$$

$$\ddot{\zeta}\left(t_{a0}\right)\left[\sigma - F_2'\left(\hat{w}\right)\right] - \left(\frac{-\hat{u}}{t_{a0}}\right)^2 F_2''\left(\hat{w}\right) = \frac{2\lambda}{t_{a0}^3}$$

$$\ddot{\zeta}\left(t_{a0}\right)\left[\sigma - F_1\left(\hat{w}\right)\right] - \left(\frac{\hat{u}}{t_{a0}}\right)^2 f\left(\hat{w}\right) = \frac{2\lambda}{t_{a0}^3}$$

$$\ddot{\zeta}\left(t_{a0}\right)\frac{\mu_f}{m_0} - \left(\frac{\hat{u}}{t_{a0}}\right)^2 f\left(\hat{w}\right) = 2\frac{z_{f0}}{t_{a0}^3}\frac{\mu_f}{m_0}$$

$$\ddot{\zeta}\left(t_{a0}\right) = \frac{z_{f0}}{t_{a0}^3}\left[2 + \frac{m_0}{\mu_f}\,\hat{u}\,f\left(\hat{w}\right)\right] = \frac{\hat{u}}{t_{a0}^2}\left[2 + \frac{m_0}{\mu_f}\,\hat{u}\,f\left(\hat{w}\right)\right].$$

20

Thus, using Eqn. 2.11,

$$\dot{v}_f\left(t_{a0}\right) = \ddot{\zeta}\left(t_{a0}\right) t_{a0} + 2\dot{\zeta}\left(t_{a0}\right) = \frac{\hat{u}}{t_{a0}^2}\left[2 + \frac{m_0}{\mu_f}\,\hat{u}\,f\left(\hat{w}\right)\right] t_{a0} - 2\frac{\hat{u}}{t_{a0}} = \frac{m_0}{\mu_f}\frac{\hat{u}^2}{t_{a0}}\,f\left(\hat{w}\right)$$

and so

$$\dot{v}_f\left(t_{a0}\right) = 0 \implies f\left(\hat{w}\right) = 0\,.$$

If an instantly created ejecta cloud is to produce a smooth-start Asay foil trajectory with $\dot{v}_f\left(t_{a0}\right) \approx 0$, the particle velocity distribution must go to zero at the maximum relative velocity. This is consistent with the combined exploratory findings plotted in Fig. 7.

This finding is closely related to boundary conditions for sustained-production ejecta source models, derived from considerations of piezoelectric pin data [3].

3.7   Final Foil Velocity

We can also derive an expression for the final foil velocity, $v_f\left(t_{fs}\right) = \dot{z}_f\left(t_{fs}\right)$. From above, and utilizing the boundary condition $\zeta\left(t_{fs}\right) = 0$,

$$v_f\left(t_{fs}\right) = \dot{\zeta}\left(t_{fs}\right) t_{fs} + \zeta\left(t_{fs}\right) + u_{fs} = \dot{\zeta}\left(t_{fs}\right) t_{fs} + u_{fs}$$

while

$$\dot{\zeta}\left(t_{fs}\right) = -\frac{\lambda}{t_{fs}^2}\frac{1}{\sigma - F_2'\left[\zeta\left(t_{fs}\right)\right]} = -\frac{\lambda}{t_{fs}^2}\frac{1}{\sigma - F_1(0)} = -\frac{\lambda}{t_{fs}^2}\frac{1}{\frac{\mu_f}{m_0} + F_1\left(\hat{w}\right) - F_1(0)}$$

$$= -\frac{\lambda}{t_{fs}^2}\frac{1}{\frac{\mu_f}{m_0} + \int_0^{\hat{w}} f(w)\,\mathrm{d}w} = -\frac{\lambda}{t_{fs}^2}\frac{1}{1 + \frac{\mu_f}{m_0}} = -\frac{z_{f0}}{t_{fs}^2}\frac{1}{1 + \frac{m_0}{\mu_f}}$$

so the final foil velocity becomes

$$v_f\left(t_{fs}\right) = u_{fs} - \frac{z_{f0}}{t_{fs}}\frac{1}{1 + \frac{m_0}{\mu_f}} = u_{fs} - \frac{u_{fs} - \frac{m_0}{\mu_f}\langle w\rangle}{1 + \frac{m_0}{\mu_f}} = \frac{\frac{m_0}{\mu_f}\left(u_{fs} + \langle w\rangle\right)}{1 + \frac{m_0}{\mu_f}} = \frac{m_0}{\mu_f + m_0}\left(\langle w\rangle + u_{fs}\right)\,.$$

This is exactly the solution (at causal measurement times) to the single-particle problem demonstrated in §2.1, with $\tilde{w} = \langle w\rangle$.

In other words, for instant-production scenarios, the final velocity of the foil is equivalent to the velocity that would be computed assuming every particle moved at the mean of the velocity distribution. This result is borne out by the analytically computed examples, above.

21

3.8 True & Inferred Cumulative Areal Masses

The true accumulated ejecta areal mass on a foil, arising from an instant-creation source function, is

$$\mu_{e,t}(t) = m_t\left[z_f(t); t\right] = m_0 \int_0^{\hat{w}} \int_0^{\frac{[w-\zeta(t)]\,t}{w}} f(w)\,\delta\left(t_c\right)\,\mathrm{d}t_c\,\mathrm{d}w = m_0 \int_{\zeta(t)}^{\hat{w}} f(w)\,\mathrm{d}w\,. \quad (3.7)$$

Given a solution for $\zeta(t)$, this is a straightforward calculation. Note the boundary conditions $\zeta\left(t_{a0}\right) = \hat{w}$ and $\zeta\left(t_{fs}\right) = 0$ yield the required values $\mu_{e,t}\left(t_{a0}\right) = 0$ and $\mu_{e,t}\left(t_{fs}\right) = m_0$, respectively.

The inferred ejecta areal mass, $\mu_{e,i}(t)$, derives from the foil trajectory, $\dot{z}_f(t)$, which is the physics quantity obtained from an Asay foil diagnostic measurement. This is achieved by solving the equation of motion for the foil, which relates μ_e and v_f.

At a given measurement time t, basic kinematics give

$$\left[\mu_f + \mu_e(t)\right] v_f(t) = \frac{1}{A} \int_{t_{a0}}^{t} F_f\left(t'\right)\,\mathrm{d}t' = \int_{t_{a0}}^{t} P_f\left(t'\right)\,\mathrm{d}t'$$

where A is the relevant collecting area of the sensor, and F_f and P_f are the force and pressure applied to the foil via inelastic momentum transfer.

The standard piezoelectric sensor analysis procedure [10] proceeds from the assumption that the ejecta cloud is sufficiently fluid that the pressure on the sensor can be treated as the dynamical ram pressure

$$P_f(t) = \rho^*(t)\,v^2(t)$$

where $\rho^*(t)$ is the dynamical cloud volume density and $v(t)$ is the time-of-flight velocity of ejecta particles arriving at time t (hence the analysis assumption of instant creation). Applying the same reasoning here yields

$$\left[\mu_f + \mu_e(t)\right] v_f(t) = \int_{t_{a0}}^{t} \rho^*\left(t'\right) v^2\left(t'\right)\,\mathrm{d}t'$$

$$\implies \mu_f\,\dot{v}_f + \mu_e\,\dot{v}_f + \dot{\mu}_e\,v_f = \rho^*\,v^2\,.$$

The piezoelectric mass inference procedure [10] is based on the relationship

$$\mu_e(t) = \int_{t_{a0}}^{t} \rho^*(t')\, v(t')\, \mathrm{d}t'$$

from which it follows

$$\mu_f\, \dot{v}_f + \mu_e\, \dot{v}_f + \dot{\mu}_e\, v_f = \dot{\mu}_e\, v\,,$$

meaning the foil equation of motion *assuming instant creation* is

$$\left[\mu_f + \mu_e(t)\right] \dot{v}_f(t) = \left[v(t) - v_f(t)\right] \dot{\mu}_e(t)\,. \tag{3.8}$$

In practice the only unknown quantity is μ_e, as μ_f is known from the construction of the foil, v is determined by the measurement time (time of flight) and assumption of instant creation, and v_f is the physics measurement.

The solution for $\mu_e(t)$ is straightforward. Let $\mu(t) \equiv \mu_f + \mu_e(t)$. Then $\dot{\mu} = \dot{\mu}_e$, so the equation of motion gives

$$\mu\, \dot{v}_f = (v - v_f)\, \dot{\mu} \implies \dot{\mu} = \frac{\dot{v}_f}{(v - v_f)}\, \mu \implies \mu(t) = \mu_0 \exp\left[\int_{t_{a0}}^{t} \frac{\dot{v}_f}{v - v_f}\, \mathrm{d}t'\right]\,.$$

At the instant of first ejecta arrival on the sensor, t_{a0}, no mass has accumulated yet, so $\mu(t_{a0}) = \mu_f$, and thus the initial condition sets $\mu_0 = \mu_f$. The exact solution to the foil equation of motion (again, assuming instant creation) is therefore

$$\mu_{e,i}(t) = \mu_f \cdot [\vartheta(t) - 1] \tag{3.9}$$

$$\vartheta(t) = \mathrm{e}^{\int_{t_{a0}}^{t} \varphi(t')\, \mathrm{d}t'}$$

$$\varphi(t) = \frac{\dot{v}_f(t)}{v(t) - v_f(t)}\,.$$

This takes a simpler and more compact form in terms of ζ. When the ejecta creation is truly instantaneous,

$$\zeta(t) \equiv \frac{z_f(t)}{t} - u_{fs} = v(t) - u_{fs} \implies v(t) = \zeta(t) + u_{fs}\,.$$

23

Using the previously derived expressions for v_f and $\dot{v}_f$ (see §2.2), we can write

$$\varphi(t) = \frac{\ddot{\zeta}\,t + 2\dot{\zeta}}{(\zeta + u_{fs}) - \left(\dot{\zeta}\,t + \zeta + u_{fs}\right)} = -\frac{\ddot{\zeta}\,t + 2\dot{\zeta}}{\dot{\zeta}\,t} = -\frac{\ddot{\zeta}}{\dot{\zeta}} - \frac{2}{t} = -\frac{\mathrm{d}}{\mathrm{d}t}\left[\ln\left(\dot{\zeta}\,t^2\right)\right]$$

and

$$\int_{t_{a0}}^{t} \varphi\left(t'\right)\,\mathrm{d}t' = \ln\left[\dot{\zeta}(t_{a0})\,t_{a0}^2\right] - \ln\left[\dot{\zeta}(t)\,t^2\right]$$

so

$$\vartheta(t) = \frac{\dot{\zeta}(t_{a0})\,t_{a0}^2}{\dot{\zeta}\,t^2} = -\frac{z_{f0}}{\dot{\zeta}\,t^2}.$$

Note

$$\vartheta\left(t_{a0}\right) = -\frac{z_{f0}}{\dot{\zeta}(t_{a0})\,t_{a0}^2} = \frac{-z_{f0}}{-z_{f0}} = 1 \implies \mu_e\left(t_{a0}\right) = \mu_f(1-1) = 0$$

$$\vartheta\left(t_{fs}\right) = -\frac{z_{f0}}{\dot{\zeta}(t_{fs})\,t_{fs}^2} = -\frac{z_{f0}}{-\frac{z_{f0}}{t_{fs}^2}\frac{1}{1+\frac{m_0}{\mu_f}}\,t_{fs}^2} = 1 + \frac{m_0}{\mu_f} \implies \mu_e\left(t_{fs}\right) = \mu_f\left[1 + \frac{m_0}{\mu_f} - 1\right] = m_0$$

thus confirming that this form of $\vartheta(t)$ generates the required values of μ_e at the initial and final measurement times.

Finally, then, given a known (measured) foil trajectory $z_f(t) = [\zeta(t) + u_{fs}]\,t$ the exact solution for the cumulative ejecta areal mass, given the assumption of instant creation, is simply

$$\boxed{\mu_{e,i}(t) = \mu_f\left[-\frac{z_{f0}}{\dot{\zeta}\,t^2} - 1\right].}$$
(3.10)

As a sanity check, we note that if this expression is correct it must be be equivalent to the true cumulative ejecta areal mass from an instant-creation source function, Eqn. 3.7. From the implicit solution for the foil trajectory in instant-creation scenarios, Eqn. 3.2, we have

$$-\frac{\lambda}{t^2} = \left[\sigma - F_2'\left(\zeta\right)\right]\dot{\zeta} = \left[\sigma - F_1\left(\zeta\right)\right]\dot{\zeta}$$

or

$$-\frac{1}{\dot{\zeta}\,t^2} = \frac{\sigma - F_1\left(\zeta\right)}{\lambda} = \frac{\frac{\mu_f}{m_0} + F_1\left(\hat{w}\right) - F_1\left(\zeta\right)}{z_{f0}\frac{\mu_f}{m_0}} = \frac{1 + \frac{m_0}{\mu_f}\int_{\zeta}^{\hat{w}} f(w)\,\mathrm{d}w}{z_{f0}}$$

24

so then

$$\mu_{e,i}(t) = \mu_f \left[z_{f0} \frac{1 + \frac{m_0}{\mu_f} \int_\zeta^{\hat{w}} f(w)\,dw}{z_{f0}} - 1 \right] = m_0 \int_\zeta^{\hat{w}} f(w)\,dw = \mu_{e,t}(t)$$

thereby agreeing with with Eqn. 3.7.

This result is consistent with earlier work on analytic solutions for piezoelectric mass measurements; there, the inferred cumulative ejecta mass is equal to the true mass when the production is truly instantaneous [2].

3.8.1 Approximate Equation of Motion

Using

$$\dot{\zeta}\,t = v_f - (\zeta + u_{fs}) \implies \dot{\zeta}\,t^2 = v_f\,t - z_f$$

we can write

$$\vartheta(t) = \frac{z_{f0}}{z_f - v_f\,t},$$

and

$$\dot{\vartheta} = \vartheta\,\varphi = \frac{z_{f0}}{z_f - v_f\,t} \cdot \frac{\dot{v}_f}{v - v_f} = \frac{z_{f0}\,\dot{v}_f}{t\,(v - v_f)^2}.$$

When the foil velocity is negligible compared to the characteristic ejecta velocity, $v_f \ll v$, and when the foil displacement is negligible so that $z_f \approx z_{f0}$ (note both limits imply $\mu_e \ll \mu_f$)

$$\dot{\mu}_e = \mu_f\,\dot{\vartheta} \approx \mu_f \frac{\dot{v}_f}{v}.$$

This approximated equation of motion is the version originally cited by Asay [4], and is commonly used in foil analyses. However, it is contingent upon the limits $\mu_e \ll \mu_f$ and $v_f \ll v$ whereas neither the full equation of motion (Eqn. 3.8) nor its solution (Eqn. 3.10) require these limits.

Given the relationship $v \approx \frac{z_{f0}}{t}$, the approximate equation of motion has the solution

$$\mu_e(t) = \frac{\mu_f}{z_{f0}} \int_{t_{a0}}^t t'\,\dot{v}_f\,(t')\,dt'.$$

25

Integrating by parts, and applying the boundary conditions $v_f(t_{a0}) = 0$ and $z_f(t_{a0}) \equiv z_{f0}$, leads to

$$\mu_e = \frac{\mu_f}{z_{f0}}(t\,v_f + z_{f0} - z_f) = \mu_f\left(1 - \frac{z_f - t\,v_f}{z_{f0}}\right)$$

so the approximate solution for inferred cumulative ejecta areal mass can be written in the very simple form

$$\mu_{e,i}^{\mathrm{approx}}(t) = \mu_f\left[1 - \frac{1}{\vartheta(t)}\right]. \tag{3.11}$$

For comparison, recall that the exact solution to the full (unapproximated) equation of motion (Eqn. 3.9) is

$$\mu_{e,i}^{\mathrm{exact}}(t) = \mu_f\left[\vartheta(t) - 1\right],$$

meaning the fractional error incurred by using the approximate solution is

$$\chi(t) = \frac{\mu_{e,i}^{\mathrm{approx}}(t) - \mu_{e,i}^{\mathrm{exact}}(t)}{\mu_{e,i}^{\mathrm{exact}}(t)} = \frac{\mu_{e,i}^{\mathrm{approx}}(t)}{\mu_{e,i}^{\mathrm{exact}}(t)} - 1 = \frac{1}{\vartheta(t)} - 1. \tag{3.12}$$

From above, the initial fractional error will be

$$\chi(t_{a0}) = \frac{1}{\vartheta(t_{a0})} - 1 = 1 - 1 = 0$$

but these solutions will diverge as material begins to accrete upon the foil, up to a maximum fractional error of

$$\chi(t_{fs}) = \frac{1}{\vartheta(t_{fs})} - 1 = \frac{1}{1 + \frac{m_0}{\mu_f}} - 1 = -\frac{1}{1 + \frac{\mu_f}{m_0}}. \tag{3.13}$$

The preceding example calculations used $\mu_f \approx 45$ mg/cm^2 (which corresponds to a 100 μm thick titanium foil) and a plausible total sourced ejecta areal mass of $m_0 = 25$ mg/cm^2 (see, e.g., [7]), meaning $\frac{\mu_f}{m_0} \approx 1.8$ or $\chi(t_{fs}) \approx -36\%$. This corresponds to a inferred final total mass of 16 mg/cm^2 as opposed to the true sourced value of 25 mg/cm^2. The exact and approximated $\mu_{e,i}(t)$ values inferred from a variety of analytically calculated foil trajectories are illustrated in Fig. 8.
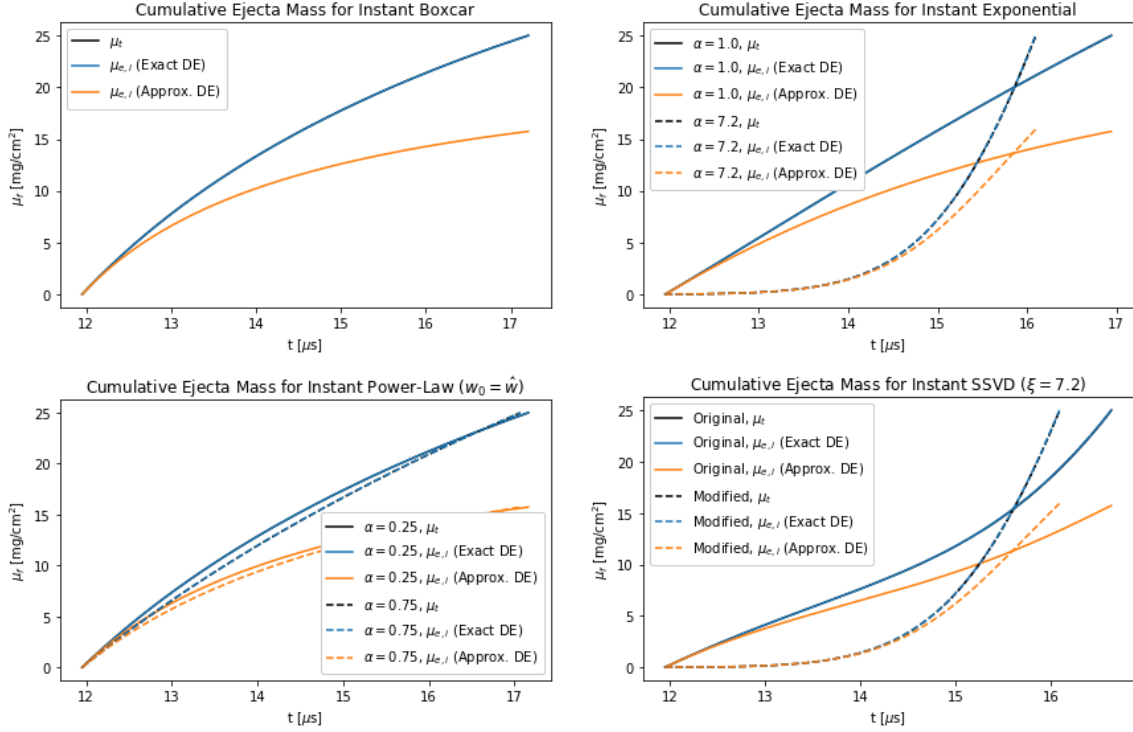
Figure 8: Cumulative ejecta areal masses corresponding to analytically derived Asay foil trajectories for instantly generated boxcar, exponential, power-law, and self-similar (original and modified) ejecta velocity distributions. These test problems used $\mu_f = 45$ mg/cm^2 (corresponding to a 100 μm thick Ti foil), a total sourced ejecta areal mass of $m_0 = 25$ mg/cm^2, a constant lab-frame free surface velocity of $u_{fs} = 1.91$ mm/μs, and a peak lab-frame ejecta velocity of $\hat{u} = 2.51$ mm/μs (these values are representative of Vogan et al. [7]). In every case, the true mass accumulation computed directly from the source function (Eqn. 3.7, black) is perfectly overlaid by the mass inferred via the exact solution to the equation of motion (Eqn. 3.10, blue). Because $m_0 \ll \mu_f$, solutions obtained from the approximated equation of motion (Eqn. 3.11, orange) are inaccurate.

A dataset analyzed using the approximate solution can be easily corrected to the exact solution. Given an inferred cumulative ejecta areal mass $\mu_{e,i}^{\text{approx}}(t)$, it follows

$$\vartheta(t) = \frac{1}{1 - \frac{\mu_{e,i}^{\text{approx}}(t)}{\mu_f}} \implies \mu_{e,i}^{\text{exact}}(t) = \frac{\mu_{e,i}^{\text{approx}}(t)}{1 - \frac{\mu_{e,i}^{\text{approx}}(t)}{\mu_f}} \; .$$

3.9 Implications for Asay Analysis Methodologies

The expression for the true mass accumulation on an Asay foil generated by an instantaneous source (Eqn. 3.7) offers an important insight into methodologies for Asay foil data analysis.

Consider two foils fielded in the same experiment. The foils may be situated at different distances from the unperturbed free surface $(z_{f0}^{(1,2)})$. Or, they could be situated at the same distance but be constructed of different materials or thicknesses; this will cause the foils to have different acceleration histories. In general,

$$\mu_e^{(1)}(t) \neq \mu_e^{(2)}(t) .$$

In fact, the ejecta arrival interval $t_{a0} \leq t < t_{fs}$ can be unique for each foil. Thus a co-plot of $\mu_e^{(1,2)}(t)$ solutions obtained via either the exact or approximate solutions will show two distinct curves when plotted as a function of t.

However, as long as the foils see the same instantly created particle distribution function, $f(w)$, Eqn. 3.7 makes it clear that

$$\mu_e^{(1)}(\zeta) = \mu_e^{(2)}(\zeta) .$$

Thus, when plotted as a function of ζ, the μ_e curves from a truly instantaneous source should lie atop each other regardless of initial distance or foil construction.

Clearly, ζ is the natural coordinate for such comparisons. But because $\zeta = v - u_{fs}$ when production is instantaneous, any co-plots calculated as a function of the time of flight ejecta velocity, v, will also align, including the often-used $\frac{v}{u_{fs}}$. However, as demonstrated in Fig. 9, *this alignment is globally true only for the exact solutions.* Mass curves computed using the approximate solution to the equation of motion will not, in general, align at higher mass values, particularly when $m_0 \lll \mu_f$.
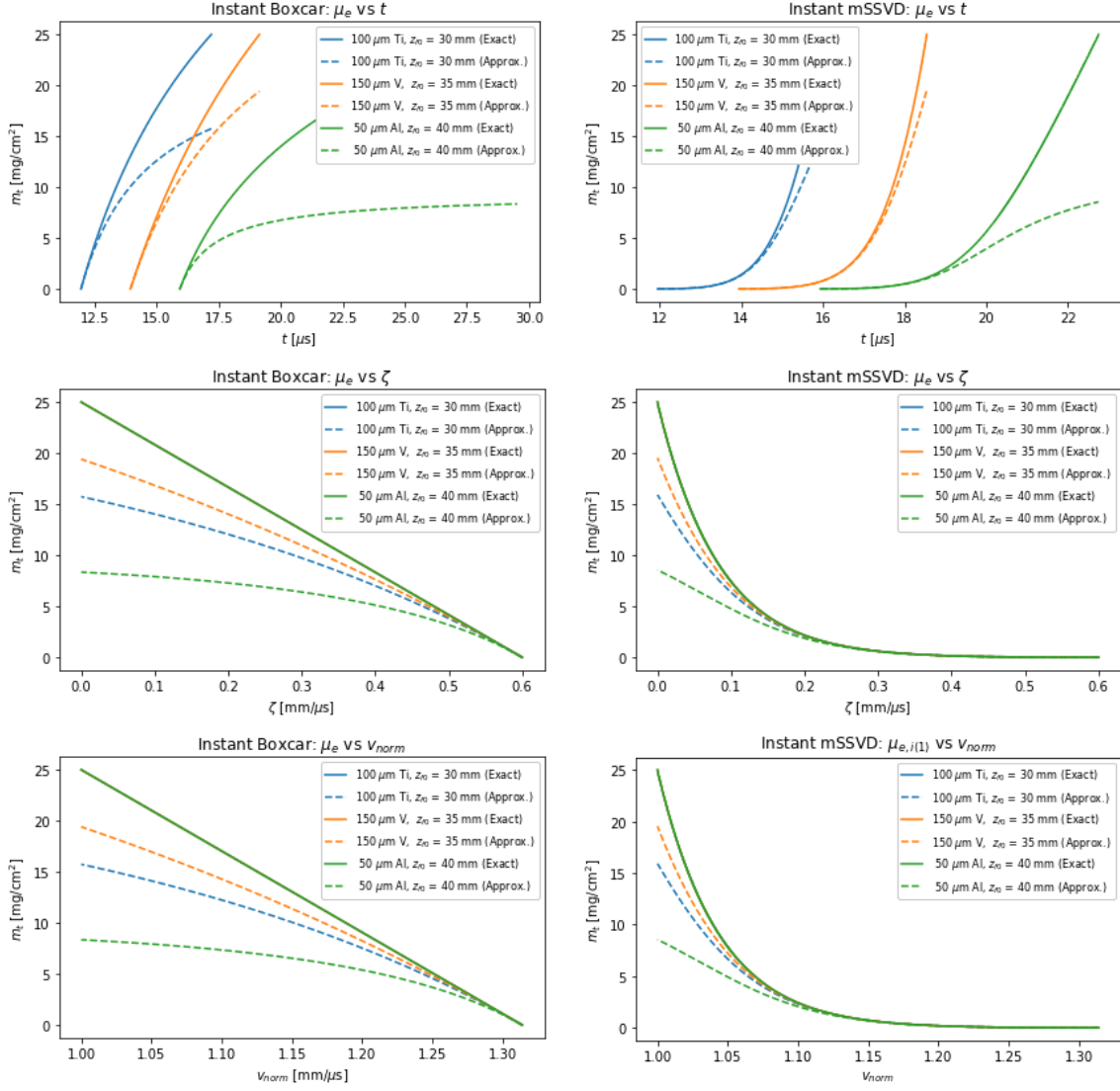
Figure 9: The cumulative ejecta areal mass $\mu_e(t)$ inferred from analytically computed foil trajectories for instant-production boxcar (left) and modified SSVD (right) velocity distributions, using $m_0 = 25$ mg/cm^2 and three different foils: 100 μm Ti, $z_{f0} = 30$ mm ($\frac{\mu_f}{m_0} \approx 1.8$) (blue); 150 μm V, $z_{f0} = 35$ mm ($\frac{\mu_f}{m_0} \approx 3.7$) (orange) ; and 50 μm Al, $z_{f0} = 40$ mm ($\frac{\mu_f}{m_0} \approx 0.54$ (green)). The masses are coplotted versus t (top), ζ (middle), $v_{norm} \equiv \frac{v}{u_{fs}}$ (bottom). The solutions computed using the exact solution (solid lines) overlay perfectly when plotted as a function of ζ or v_{norm}, even when the measurement time domain differs. This is not true for the approximate solutions (dashed lines).

29

4 Towards a Solution for Sustained Production

The existence of a closed-form solution for the foil trajectory under instant production suggests a path toward constructing a solution for more general, sustained-production sources, particularly those of the form

$$m_c(w, t_c) = m_0 f(w) g(t_c). \tag{4.1}$$

The strategy is to first extend the instant-production solution to a source represented by a train of discrete delta functions (a "Dirac comb"), and then examine the behavior of that solution in the limit that the interval between individual delta functions becomes infinitesimal (i.e., in the limit that the Dirac comb becomes a continuous function). In this way, the goal is to treat the instant-production solution a bit like a Green's function for the problem.

4.1 Time-Shifted Delta Function

Consider a source function comprising a *time-shifted* instant-production scenario

$$m_c(w, t_c) = m_0 f(w) \delta(t_c - t_0) \tag{4.2}$$

with $t_0 \neq 0$. Repeating the derivation of §2.2 for the case of a nonzero shock breakout time leads to the "affine" compact IDE

$$\dot{\zeta} \left[\mu_f + \int_0^{\hat{w}} \int_0^{\frac{(w-\zeta)t + \zeta t_0}{w}} m_c(w, t_c) \, \mathrm{d}t_c \, \mathrm{d}w \right] = -\frac{\mu_f \, z_{f0}}{(t - t_0)^2}. \tag{4.3}$$

When this version of the IDE is applied to the time-shifted instant production source, the integration over creation times (t_c) will be nonzero as long as

$$\frac{(w - \zeta)\, t + \zeta\, t_0}{w} > t_0 \implies w > \zeta$$

given that causality will ensure $t > t_0$ for all measurement times t.

Similarly to the derivation of the instant-production solution, we then obtain

$$\frac{\mu_f}{m_0}\dot\zeta + \dot\zeta \int\limits_{\zeta}^{\hat w} f(w)\,\mathrm{d}w = -\frac{\mu_f}{m_0}\frac{z_{f0}}{(t-t_0)^2}$$

$$\frac{\mu_f}{m_0}\dot\zeta + \dot\zeta\, F_1\left(\hat w\right) - \dot\zeta\, F_1\left(\zeta\right) = -\frac{\mu_f}{m_0}\frac{z_{f0}}{(t-t_0)^2}$$

$$\left[\frac{\mu_f}{m_0} + F_1\left(\hat w\right)\right]\dot\zeta - \frac{\mathrm{d}}{\mathrm{d}t}F_2\left(\zeta\right) = z_{f0}\frac{\mu_f}{m_0}\frac{\mathrm{d}}{\mathrm{d}t}\left[\frac{1}{(t-t_0)}\right]$$

$$\sigma_0\,\zeta - F_2\left(\zeta\right) = \frac{\lambda_0}{(t-t_0)} - \kappa$$

where as usual κ is a constant of integration. Now the time of first ejecta arrival at the sensor is $t_1 + \frac{z_{f0}}{\hat u} \equiv t_1 + t_{a0}$, so based on the original initial condition derivation, this problem has $\zeta\left(t_1 + t_{a0}\right) = \hat w$, which leads to $\kappa = \nu_0$ as derived previously. The implicit solution for this time-shifted scenario is therefore

$$t = t_0 + \frac{\lambda_0}{\sigma_0\,\zeta - F_2\left[\zeta\right] + \nu_0}\,. \tag{4.4}$$

Given that the second term on the right side is already known to generate times in the causal regime $t_{a0} \le t \le t_{fs}$, this solution for the time-shifted source function automatically has the correct time domain, $t_0 + t_{a0} \le t \le t_0 + t_{fs}$. Furthermore, the definition of the generalized ejecta velocity in Eqn. 2.7 gives

$$z_f(t) = \left(\zeta + u_{fs}\right)\left(t - t_0\right) = \frac{\lambda_0\left(\zeta + u_{fs}\right)}{\sigma_0\,\zeta - F_2\left[\zeta\right] + \nu_0} \qquad t_0 + t_{a0} \le t \le t_0 + t_{fs}$$

which is the expected time-shifted copy of the $t_0 = 0$ trajectory

$$z_f(t) = \left(\zeta + u_{fs}\right) t = \frac{\lambda_0\left(\zeta + u_{fs}\right)}{\sigma_0\,\zeta - F_2\left[\zeta\right] + \nu_0} \qquad t_{a0} \le t \le t_{fs}\,.$$

4.2 Two-Pulse Source Function

Now consider a source function comprising two pulses of instant production, sharing the same velocity distribution but separated by a finite time delay:

$$\begin{aligned}m_c\left(w, t_c\right) &= m_0\, f\left(w\right)\delta\left(t_c - t_0\right) + m_1\, f\left(w\right)\delta\left(t_c - t_1\right)\\ &= m_0\, f\left(w\right)\delta\left(t_c\right) + m_1\, f\left(w\right)\delta\left(t_c - t_1\right)\end{aligned} \tag{4.5}$$

where in general $t_1 > 0$. Going forward, we'll use $\lambda_k, \nu_k, \sigma_k$ to denote constants containing a mass normalization constant m_k, and use non-subscripted symbols λ, ν, σ to denote constants normalized by the total (maximum) areal mass in the problem, $m \equiv m_0 + m_1$.

We will take it for granted, based on a wealth of experimental observations [6, 7, 10], that the velocity distribution $f(w)$ covers the domain $(0, \hat{w}]$, meaning the trajectory solution will naturally break into two regimes. At sufficiently early times, only particles created in the m_0 pulse can reach the foil, but eventually a mixture of particles generated in both pulses will reach the moving sensor. More concretely, these regimes are

1. $t_{a0} = \frac{z_{f0}}{\hat{u}} \leq t < t_{a1}$

2. $t_{a1} \leq t \leq t_{fs}$

where t_{a1} is the *unknown* time at which particles from the m_1 pulse begin to arrive on the accelerated foil, and t_{fs} is the *unknown* time of free surface arrival at the foil. The value of t_{a1} is implicitly defined by the important relationship

$$u_{fs}\,(t_1 - t_0) + \hat{u}\,(t_{a1} - t_1) = z_f\,(t_{a1})$$
$$\hat{u}\,t_{a1} - \hat{w}\,t_1 = [\zeta\,(t_{a1}) + u_{fs}]\,t_{a1}$$
$$\hat{w}\,(t_{a1} - t_1) = t_{a1}\,\zeta\,(t_{a1})$$
$$\implies \hat{w}\left(1 - \frac{t_1}{t_{a1}}\right) = \zeta\,(t_{a1})\ . \tag{4.6}$$

Regime 1 constitutes our original instant-production scenario, so there the implicit solution for the trajectory must be

$$t = \frac{\lambda_0}{\sigma_0\,\zeta - F_2\,[\zeta] + \nu_0}\ . \tag{4.7}$$

Our focus is to find a general solution for Regime 2, as at that point we will have the full solution for this problem. We already know, based on the preceding analyses, that the Regime 2 solution must exhibit particular limits:

$$m_1 \to 0 \implies t = \frac{\lambda_0}{\sigma_0\,\zeta - F_2\,[\zeta] + \nu_0} \tag{4.8}$$
$$t_1 \to 0 \implies t = \frac{\lambda}{\sigma\,\zeta - F_2\,[\zeta] + \nu} \tag{4.9}$$

32

However, and very importantly,

$$m_0 \to 0 \implies t = t_1 + \frac{\lambda_1}{\sigma_1 \, \zeta - F_2 \, [\zeta] + \nu_1} \, .$$

The reason this limit shouldn't recover the time-shifted solution from §4.1 is because in that problem definition, shock breakout and ejecta production were time-shifted from $t_0 = 0$ while still coincident. Here, the existence of two separate delta functions at $t_0 = 0$ and $t_1 > 0$ fixes the shock breakout at t_0, meaning the "clock" starts running before the ejecta production pulse at t_1, even when $m_0 \to 0$. This is an intermediate step toward considering double-shock scenarios, where the free surface is shocked (and accelerated) twice, with a potentially different velocity distribution generated in each event. Here, the surface is not reaccelerated, and the pulses generate the same particle velocity distribution.

Two final preparatory observations are

$$\int_0^{\hat{w}} w^n f(w) \int_0^{\frac{(w-\zeta)\,t}{w}} \delta\,(t_c) \, \mathrm{d}t_c \, \mathrm{d}w = \int_\zeta^{\hat{w}} w^n f(w) \, \mathrm{d}w$$

$$\int_0^{\hat{w}} w^n f(w) \int_0^{\frac{(w-\zeta)\,t}{w}} \delta\,(t_c - t_1) \, \mathrm{d}t_c \, \mathrm{d}w = \int_{\frac{\zeta t}{t-t_1}}^{\hat{w}} w^n f(w) \, \mathrm{d}w \,,$$

and

$$\int_a^b w \, f(w) \, \mathrm{d}w = \int_a^b w \, F_1'(w) \, \mathrm{d}w = w \, F_1(w) \Big|_a^b - \int_a^b F_1(w) \, \mathrm{d}w = \left[w \, F_1(w) - F_2(w) \right] \Big|_a^b \, .$$

Placing the source AMF for this problem, Eqn. 4.5, into the noncompact IDE

(Eqn. 2.13) therefore yields

$$
\mu_f\, u_{fs} + \mu_f\left(\dot\zeta\, t + \zeta\right) + \left(\dot\zeta\, t + \zeta\right)\left[m_0 \int_{\zeta}^{\hat w} f(w)\,\mathrm{d}w + m_1 \int_{\frac{\zeta t}{t-t_1}}^{\hat w} f(w)\,\mathrm{d}w \right] =
$$
$$
m_0 \int_{\zeta}^{\hat w} w\, f(w)\,\mathrm{d}w + m_1 \int_{\frac{\zeta t}{t-t_1}}^{\hat w} w\, f(w)\,\mathrm{d}w
$$

or, after combining terms on the left side,

$$
\mu_f\, u_{fs} + \left[\mu_f + m\, F_1\left(\hat w\right)\right]\left(\dot\zeta\, t + \zeta\right) - m_0\left(\dot\zeta\, t + \zeta\right) F_1(\zeta) - m_1\left(\dot\zeta\, t + \zeta\right) F_1\left(\frac{\zeta t}{t-t_1}\right) =
$$
$$
m_0\left[\hat w\, F_1\left(\hat w\right) - F_2\left(\hat w\right) - \zeta\, F_1\left(\zeta\right) - F_2\left(\zeta\right)\right] +
$$
$$
m_1\left[\hat w\, F_1\left(\hat w\right) - F_2\left(\hat w\right) - \left(\frac{\zeta t}{t-t_1}\right) F_1\left(\frac{\zeta t}{t-t_1}\right) + F_2\left(\frac{\zeta t}{t-t_1}\right)\right]
$$

and after a little more algebra,

$$
\left[\mu_f\, u_{fs} + m\, F_2\left(\hat w\right) - m\, \hat w\, F_1\left(\hat w\right)\right] + \left[\mu_f + m\, F_1\left(\hat w\right)\right]\left(\dot\zeta\, t + \zeta\right)
$$
$$
+ m_0\left[\zeta\, F_1(\zeta) - \left(\dot\zeta\, t + \zeta\right) F_1(\zeta) - F_2(\zeta)\right]
$$
$$
+ m_1\left[\left(\frac{\zeta t}{t-t_1}\right) F_1\left(\frac{\zeta t}{t-t_1}\right) - \left(\dot\zeta\, t + \zeta\right) F_1\left(\frac{\zeta t}{t-t_1}\right) - F_2\left(\frac{\zeta t}{t-t_1}\right)\right] = 0 .
$$

Dividing by $m \equiv m_0 + m_1$ leads to the more manageable form

$$
\nu + \sigma\left(\dot\zeta\, t + \zeta\right) + \frac{m_0}{m}\left[\zeta\, F_1(\zeta) - \left(\dot\zeta\, t + \zeta\right) F_1(\zeta) - F_2(\zeta)\right]
$$
$$
+ \frac{m_1}{m}\left[\left(\frac{\zeta t}{t-t_1}\right) F_1\left(\frac{\zeta t}{t-t_1}\right) - \left(\dot\zeta\, t + \zeta\right) F_1\left(\frac{\zeta t}{t-t_1}\right) - F_2\left(\frac{\zeta t}{t-t_1}\right)\right] = 0 .
$$
$$
(4.10)
$$

Additional simplification can be obtained from the relations

$$
\left[\zeta\, F_1(\zeta) - \left(\dot\zeta\, t + \zeta\right) F_1(\zeta) - F_2(\zeta)\right] = -\frac{\mathrm{d}}{\mathrm{d}t}\left[t\, F_2(\zeta)\right]
$$
$$
\left[\left(\frac{\zeta t}{t-t_1}\right) F_1\left(\frac{\zeta t}{t-t_1}\right) - \left(\dot\zeta\, t + \zeta\right) F_1\left(\frac{\zeta t}{t-t_1}\right) - F_2\left(\frac{\zeta t}{t-t_1}\right)\right] = -\frac{\mathrm{d}}{\mathrm{d}t}\left[(t-t_1)\, F_2\left(\frac{\zeta t}{t-t_1}\right)\right]
$$

34

such that we can write

$$\nu + \sigma \frac{\mathrm{d}}{\mathrm{d}t}\left(\zeta\, t\right) - \frac{m_0}{m}\frac{\mathrm{d}}{\mathrm{d}t}\left[t\, F_2(\zeta)\right] - \frac{m_1}{m}\frac{\mathrm{d}}{\mathrm{d}t}\left[(t - t_1)\, F_2\left(\frac{\zeta t}{t - t_1}\right)\right] = 0\,.$$

It's worth pointing out, for future reference, that because

$$t\, F_2(\zeta) = (t - t_0)\, F_2\left(\frac{\zeta t}{t - t_0}\right)$$

this could be written in the form

$$\nu + \sigma \frac{\mathrm{d}}{\mathrm{d}t}\left(\zeta\, t\right) - \sum_{i=0}^{1}\frac{m_i}{m}\frac{\mathrm{d}}{\mathrm{d}t}\left[(t - t_i)\, F_2\left(\frac{\zeta t}{t - t_i}\right)\right] = 0\,. \tag{4.11}$$

Integration by t yields

$$\nu\, t + \sigma\,(\zeta\, t) - \frac{m_0}{m}\left[t\, F_2(\zeta)\right] - \frac{m_1}{m}\left[(t - t_1)\, F_2\left(\frac{\zeta t}{t - t_1}\right)\right] = \kappa$$

where κ is a (currently unknown) constant of integration. Because Regime 2 is defined such that $t \geq t_{a1} > t_{a0} > 0$, we can divide through by t to obtain, finally, the governing equation for Regime 2:

$$\sigma\,\zeta + \nu - \frac{m_0}{m}\, F_2(\zeta) - \frac{m_1}{m}\left(\frac{t - t_1}{t}\right)\, F_2\left(\frac{\zeta t}{t - t_1}\right) = \frac{\kappa}{t} \tag{4.12}$$

where

$$\sigma \equiv \frac{\mu_f}{m} + F_1\left(\hat{w}\right)$$

$$\nu \equiv \left(\frac{\mu_f}{m}\right)u_{fs} + F_2\left(\hat{w}\right) - \hat{w}\, F_1\left(\hat{w}\right)$$

$$m \equiv m_0 + m_1 = \sum_{i=0}^{1} m_i\,.$$

4.2.1 $m_1 \to 0$

When $m_1 \to 0$, $m \to m_0$ in which case Eqn. 4.12 will obviously become

$$\sigma_0\,\zeta - F_2(\zeta) + \nu_0 = \frac{\kappa}{t}$$

35

and because $t = t_{a0}$ falls within the domain, applying the initial condition $\zeta(t_{a0}) = \hat{w}$ leads to $\kappa = \lambda_0$ per the derivation in §3, thereby generating the previously identified solution required in this particular limit:

$$t = \frac{\lambda_0}{\sigma_0\,\zeta - F_2\,[\zeta] + \nu_0}\,.$$

4.2.2 $t_1 \to 0$

Similarly, when $t_1 \to 0$, Eqn. 4.12 will become

$$\sigma\,\zeta - F_2(\zeta) + \nu = \frac{\kappa}{t}$$

and the $\zeta(t_{a0})$ initial condition will yield $\kappa = \lambda$, thereby generating the previously identified solution required for this limit, too:

$$t = \frac{\lambda}{\sigma\,\zeta - F_2\,[\zeta] + \nu}\,.$$

4.2.3 $m_0 \to 0$

Now consider $m_0 \to 0$. In this limit, Eqn. 4.12 will become

$$\sigma_1\,\zeta - \left(\frac{t - t_1}{t}\right) F_2\left(\frac{\zeta t}{t - t_1}\right) + \nu_1 = \frac{\kappa}{t}$$

or

$$\sigma_1\left(\frac{\zeta t}{t - t_1}\right) - F_2\left(\frac{\zeta t}{t - t_1}\right) + \nu_1\left(\frac{t}{t - t_1}\right) = \frac{\kappa}{t - t_1}$$

and the domain of the problem will be $t_{a1} \le t \le t_{fs}$. Now it is possible to solve exactly for the first arrival time, t_{a1}:

$$u_{fs}\,(t_1 - t_0) + \hat{u}\,(t_{a1} - t_1) = z_{f0} \implies t_{a1} = \frac{z_{f0} + \hat{w}\,t_1}{\hat{u}} = t_{a0} + \frac{\hat{w}\,t_1}{\hat{u}}\,.$$

It is straightforward to show this value preserves the previously derived relationship $\zeta(t_{a1}) = \hat{w}$, from which it also follows

$$\hat{w} \ge \frac{\zeta\,t}{t - t_1} \ge 0 \qquad \text{for} \qquad t_{a1} \le t \le t_{fs}$$

36

because the boundary condition $\zeta(t_{fs}) = 0$ still applies. When $t = t_{a1}$ the governing equation in this $m_0 \to 0$ limit becomes

$$\kappa = (t_{a1} - t_1) \left[\sigma_1 \hat{w} - F_2(\hat{w}) \right] + t_{a1} \nu_1$$

from which it follows, after a little algebra,

$$\kappa = \lambda_1 + t_1 \left[F_2(\hat{w}) - \hat{w} F_1(\hat{w}) \right].$$

Written in terms of the natural variable $y \equiv \frac{\zeta t}{t - t_1}$ the governing equation for this $m_0 \to 0$ limiting case becomes

$$\sigma_1 y (t - t_1) - F_2(y) (t - t_1) + \nu_1 t = \lambda_1 + t_1 \left[F_2(\hat{w}) - \hat{w} F_1(\hat{w}) \right]$$
$$\sigma_1 y (t - t_1) - F_2(y) (t - t_1) + \nu_1 (t - t_1) = \lambda_1 + t_1 \left[F_2(\hat{w}) - \hat{w} F_1(\hat{w}) - \nu_1 \right]$$
$$(t - t_1) \left[\sigma_1 - F_2(y) + \nu_1 \right] = \lambda_1 - \left(\frac{\mu_f}{m_1} \right) u_{fs} t_1$$

so the implicit trajectory solution for the $m_0 \to 0$ limit of the two-pulse problem is

$$t = t_1 + \frac{\lambda_1 - \left(\frac{\mu_f}{m_1} \right) u_{fs} t_1}{\sigma_1 y - F_2(y) + \nu_1}$$

where the foil position is given by

$$z_f(t) = \left[\zeta(t) + u_{fs} \right] (t - t_0) = \left[\left(\frac{t - t_1}{t} \right) y + u_{fs} \right] t.$$

Now the implicit solution gives $t(y)$ for $\hat{w} \geq y \geq 0$.

As a sanity check, we furthermore note that when $y = \hat{w}$, this implicit solution gives

$$t = t_1 + \frac{\lambda_1 - \left(\frac{\mu_f}{m_1} \right) u_{fs} t_1}{\sigma_1 \hat{w} - F_2(\hat{w}) + \nu_1} = t_1 + \frac{\lambda_1 - \left(\frac{\mu_f}{m_1} \right) u_{fs} t_1}{\left(\frac{\mu_f}{m_1} \right) \hat{u}} = t_1 + \frac{\left(\frac{\mu_f}{m_1} \right) (z_{f0} - u_{fs} t_1)}{\left(\frac{\mu_f}{m_1} \right) \hat{u}}$$
$$= \frac{z_{f0} + \hat{w} t_1}{\hat{u}} = t_{a0} + \frac{\hat{w} t_1}{\hat{u}}$$

thereby agreeing with the expression for t_{a1} obtained directly, above. (Notice the delay relative to t_{a0} is not simply t_1, as one might be tempted to assume.) Applying

the boundary condition $\zeta\left(t_{fs}\right) = 0 \implies y\left(t_{fs}\right) = 0$ yields

$$t_{fs} = t_1 + \frac{\lambda_1 - \left(\frac{\mu_f}{m_1}\right) u_{fs}\, t_1}{\nu_1 - F_2(0)} = \frac{\lambda_1}{\nu_1 - F_2(0)} + \frac{t_1\left[\nu_1 - F_2(0) - \left(\frac{\mu_f}{m_1}\right) u_{fs}\right]}{\nu_1 - F_2(0)}$$

$$= \frac{\lambda_1}{\nu_1 - F_2(0)} + \frac{t_1\left[F_2\left(\hat{w}\right) - F_2(0) - \hat{w}\, F_1\left(\hat{w}\right)\right]}{\nu_1 - F_2(0)}$$

$$= \frac{\lambda_1}{\nu_1 - F_2(0)} - \frac{t_1 \int\limits_0^{\hat{w}} w\, f(w)\, \mathrm{d}w}{\nu_1 - F_2(0)}$$

$$= \frac{\lambda_1}{\nu_1 - F_2(0)} - \frac{t_1\,\langle w\rangle}{\nu_1 - F_2(0)}.$$

The first term is the t_{fs} value pertaining to the source function $m_c\left(w, t_c\right) = m_1\, f(w)\, \delta\left(t_c\right)$. Notice how the full solution for this $m_0 \to 0$ scenario has a later first-arrival time yet an *earlier* free-surface arrival time than in the associated single-pulse scenario: here the free surface approaches the motionless foil throughout the interval $t_0 \le t \le t_1$ yet ejecta production doesn't begin until t_1.

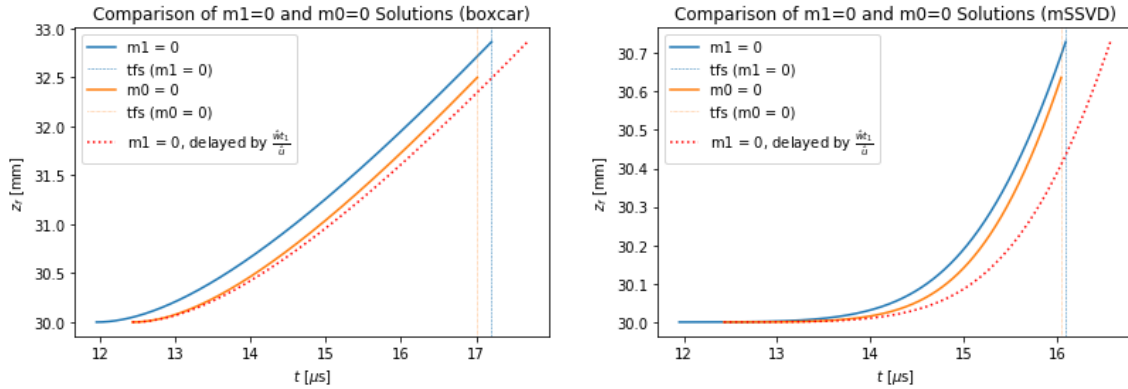As illustrated in Fig. 10, the solution for $m_0 \to 0$ is not simply a time-shifted version of the solution for $m_1 \to 0$.

Figure 10: Example trajectory solutions $[z_f(t)]$ for the $m_1 \to 0$ and $m_0 \to 0$ limits of the two-pulse source function. As with previous examples, these calculations used ejecta parameter values representative of Vogan et al. [7]: $m_{0,1} = 25$ mg/cm^2, $u_{fs} = 1.91$ mm/μs, $\hat{u} = 2.51$ mm/μs. The trajectories pertain to a 100 μm thick Ti foil ($\mu_f = 45$ mg/cm^2), and the delay between pulses was $t_1 = 2$ μs. Left: boxcar velocity distribution. Right: modified SSVD.

38

4.2.4 General Solution: $m_0 \neq 0$, $m_1 \neq 0$, $t_1 \neq 0$

The governing equation for Regime 2 (Eqn. 4.12) can be written

$$\sigma \zeta + \nu - \left(\frac{m_0}{m}\right) F_2(\zeta) - \left(\frac{m_1}{m}\right) F_2\left(\frac{\zeta t}{t - t_1}\right) + \left(\frac{t_1}{t}\right)\left(\frac{m_1}{m}\right) F_2\left(\frac{\zeta t}{t - t_1}\right) = \frac{\kappa}{t}$$

$$t\left[\sigma \zeta + \nu - \left(\frac{m_0}{m}\right) F_2(\zeta) - \left(\frac{m_1}{m}\right) F_2\left(\frac{\zeta t}{t - t_1}\right)\right] + \left(\frac{t_1 m_1}{m}\right) F_2\left(\frac{\zeta t}{t - t_1}\right) = \kappa$$

so the general implicit solution for Regime 2 is

$$t = \frac{\kappa - \left(\dfrac{t_1 m_1}{m}\right) F_2\left(\dfrac{\zeta t}{t - t_1}\right)}{\sigma \zeta + \nu - \left(\dfrac{m_0}{m}\right) F_2(\zeta) - \left(\dfrac{m_1}{m}\right) F_2(y)} \qquad (4.13)$$

where, as before, we've used $y \equiv \frac{\zeta t}{t - t_1}$. The presence of y on the right-hand side complicates the implicit solution for $t(\zeta)$: in general, this will have to be solved numerically.

The value of κ is determined by the requirement that the solutions for Regime 1 and Regime 2 join smoothly at $t = t_{a1}$. The value of t_{a1} can be obtained by numerically solving Eqn. 4.6, at which point the Regime 1 solution gives us $\zeta(t_{a1}) \equiv \zeta_{a1}$. Equating the Regime 1 and Regime 2 solutions at this time, and using $y(t_{a1}) = \hat{w}$, yields

$$t_{a1} = \frac{\kappa - \left(\dfrac{t_1 m_1}{m}\right) F_2(\hat{w})}{\sigma \zeta_{a1} + \nu - \left(\dfrac{m_0}{m}\right) F_2(\zeta_{a1}) - \left(\dfrac{m_1}{m}\right) F_2(\hat{w})}$$

or

$$\kappa = \left[\sigma \zeta_{a1} + \nu - \left(\frac{m_0}{m}\right) F_2(\zeta_{a1})\right] t_{a1} - (t_{a1} - t_1)\left(\frac{m_1}{m}\right) F_2(\hat{w}).$$

When $\zeta = y = 0$, Eqn. 4.13 yields

$$t_{fs} = \frac{\kappa - \left(\dfrac{t_1 m_1}{m}\right) F_2(0)}{\nu - F_2(0)}.$$

In summary, the full implicit solution for this two-pulse source function is

$$t = \begin{cases} \dfrac{\lambda_0}{\sigma_0\,\zeta - F_2\left(\zeta\right) + \nu_0} & t_{a0} = \frac{z_{f0}}{\hat{u}} \leq t < t_{a1} \\[3em] \dfrac{\kappa - \left(\dfrac{t_1\,m_1}{m}\right) F_2\left(\dfrac{\zeta\,t}{t - t_1}\right)}{\sigma\,\zeta + \nu - \left(\dfrac{m_0}{m}\right) F_2(\zeta) - \left(\dfrac{m_1}{m}\right) F_2(y)} & t_{a1} \leq t < t_{fs} \end{cases} \tag{4.14}$$

where the constants, t_{a1}, and t_{fs} are as defined above. Example solutions are shown in Fig. 11.
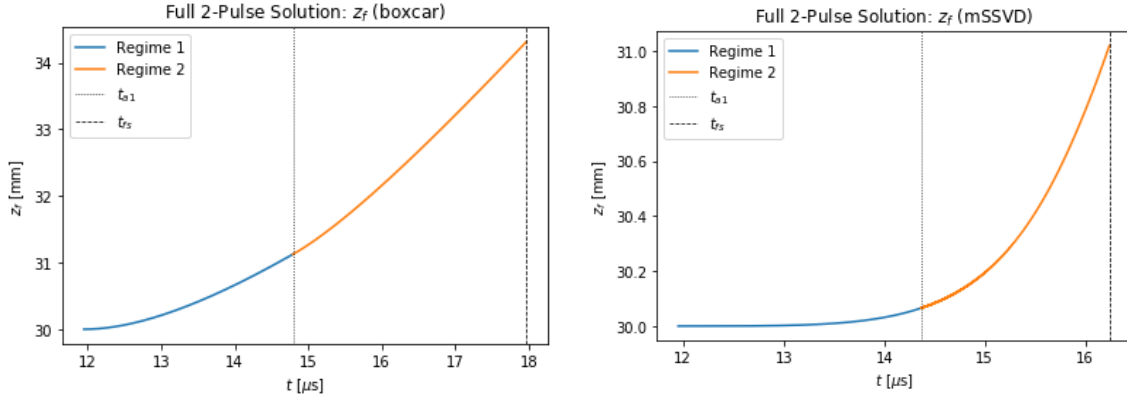

Figure 11: Example trajectory solutions $[z_f(t)]$ for the full two-pulse source function, for boxcar (left) and modified SSVD (right) distributions. As with previous examples, these calculations used ejecta parameter values representative of Vogan et al. [7]: $m_{0,1} = 25$ mg/cm^2, $u_{fs} = 1.91$ mm/μs, $\hat{u} = 2.51$ mm/μs. The trajectories pertain to a 100 μm thick Ti foil ($\mu_f = 45$ mg/cm^2). To help emphasize the separate regimes, the delay between pulses was arbitrarily set to a very large $t_1 = 10$ μs.

4.3   Dirac Comb

We now generalize the two-pulse source function to a train of N pulses, namely a Dirac comb:

$$m_c\left(w, t_c\right) = \sum_{n=0}^{N} m_n\, f(w)\, \delta\left(t_c - t_n\right) \tag{4.15}$$

40

where as usual $t_0 = 0$. For future convenience, let us also define

$$M_j \equiv \sum_{n=0}^{j} m_n \,.$$

The trajectory solution now has $N + 1$ regimes, where regime j corresponds to the time domain $t_{a\,(j-1)} \leq t < t_{a\,j}$ and $t_{a\,j}$ is the time of first arrival at the sensor for particles created in the m_j pulse. The trajectory solution for Regime 1 is the familiar single-pulse instant production solution derived and explored in §3.

Consider regime $k + 1$, for $1 < k \leq N$. The derivation of the implicit equation for the foil trajectory follows much as in §4.2. Placing the Dirac comb source function into the noncompact IDE (Eqn. 2.13) yields:

$$\mu_f\, u_{fs} + \mu_f \left(\dot{\zeta}\, t + \zeta \right) + \left(\dot{\zeta}\, t + \zeta \right) \sum_{n=0}^{k} m_n \int_0^{\hat{w}} f(w) \int_0^{\frac{(w-\zeta)\,t}{\zeta}} \delta\left(t_c - t_n\right) \mathrm{d}t_c\, \mathrm{d}w =$$

$$\sum_{n=0}^{k} m_n \int_0^{\hat{w}} w\, f(w) \int_0^{\frac{(w-\zeta)\,t}{\zeta}} \delta\left(t_c - t_n\right) \mathrm{d}t_c\, \mathrm{d}w$$

$$\mu_f\, u_{fs} + \mu_f \left(\dot{\zeta}\, t + \zeta \right) + \left(\dot{\zeta}\, t + \zeta \right) \sum_{n=0}^{k} m_n \int_{\frac{\zeta\,t}{t-t_n}}^{\hat{w}} f(w)\, \mathrm{d}w = \sum_{n=0}^{k} m_n \int_{\frac{\zeta\,t}{t-t_n}}^{\hat{w}} w\, f(w)\, \mathrm{d}w$$

$$\mu_f\, u_{fs} + \mu_f \left(\dot{\zeta}\, t + \zeta \right) + \left(\dot{\zeta}\, t + \zeta \right) \sum_{n=0}^{k} m_n \left[F_1\left(\hat{w}\right) - F_1\left(\frac{\zeta\,t}{t-t_n} \right) \right] =$$

$$\sum_{n=0}^{k} m_n \left[\hat{w}\, F_1\left(\hat{w}\right) - F_2\left(\hat{w}\right) - \left(\frac{\zeta\,t}{t-t_n} \right) F_1\left(\frac{\zeta\,t}{t-t_n} \right) + F_2\left(\frac{\zeta\,t}{t-t_n} \right) \right]$$

or, after collecting like terms,

$$\left[\mu_f\, u_{fs} + \sum_{n=0}^{k} m_n\, F_2\left(\hat{w}\right) - \sum_{n=0}^{k} m_n\, \hat{w}\, F_1\left(\hat{w}\right) \right] + \left[\mu_f + \sum_{n=0}^{k} m_n\, F_1\left(\hat{w}\right) \right] \left(\dot{\zeta}\, t + \zeta \right)$$

$$+ \sum_{n=0}^{k} m_n \left[\left(\frac{\zeta\,t}{t-t_n} \right) F_1\left(\frac{\zeta\,t}{t-t_n} \right) - \left(\dot{\zeta}\, t + \zeta \right) F_1\left(\frac{\zeta\,t}{t-t_n} \right) - F_2\left(\frac{\zeta\,t}{t-t_n} \right) \right] = 0 \,.$$

41

Now we use

$$\left(\frac{\zeta t}{t - t_n}\right) F_1\left(\frac{\zeta t}{t - t_n}\right) - \left(\dot{\zeta} t + \zeta\right) F_1\left(\frac{\zeta t}{t - t_n}\right) - F_2\left(\frac{\zeta t}{t - t_n}\right) = -\frac{\mathrm{d}}{\mathrm{d}t}\left[(t - t_n)\, F_2\left(\frac{\zeta t}{t - t_n}\right)\right]$$

and the preceding definitions to write

$$\left[\mu_f\, u_{fs} + M_k\, F_2\left(\hat{w}\right) - M_k\, \hat{w}\, F_1\left(\hat{w}\right)\right] + \left[\mu_f + M_k\, F_1\left(\hat{w}\right)\right]\left(\dot{\zeta} t + \zeta\right)$$
$$- \sum_{n=0}^{k} m_n \frac{\mathrm{d}}{\mathrm{d}t}\left[(t - t_n)\, F_2\left(\frac{\zeta t}{t - t_n}\right)\right] = 0\,.$$

Defining the usual constants

$$\nu_k \equiv \left(\frac{\mu_f}{M_k}\right) u_{fs} + F_2\left(\hat{w}\right) - \hat{w}\, F_1\left(\hat{w}\right)$$

$$\sigma_k \equiv \left(\frac{\mu_f}{M_k}\right) + F_1\left(\hat{w}\right)$$

enables us to write

$$\nu_k + \sigma_k \frac{\mathrm{d}}{\mathrm{d}t}\left(\zeta t\right) - \sum_{n=0}^{k} \frac{m_n}{M_k} \frac{\mathrm{d}}{\mathrm{d}t}\left[(t - t_n)\, F_2\left(\frac{\zeta t}{t - t_n}\right)\right] = 0\,,$$

which after integration over t becomes

$$\nu_k\, t + \sigma_k\, (\zeta t) - \sum_{n=0}^{k} \frac{m_n}{M_k}\, (t - t_n)\, F_2\left(\frac{\zeta t}{t - t_n}\right) = \kappa_k$$

where κ_k is the usual integration constant. As the time domain of Regime $k+1$ has $t > t_0 = 0$, we can divide by t to obtain the governing equation for the foil trajectory in Regime $k+1$:

$$\nu_k + \sigma_k\, \zeta - \sum_{n=0}^{k} \frac{m_n}{M_k}\left(\frac{t - t_n}{t}\right) F_2\left(\frac{\zeta t}{t - t_n}\right) = \frac{\kappa_k}{t}\,. \tag{4.16}$$

This can be cast into a form similar to our previous implicit solutions, via

$$\nu_k + \sigma_k\, \zeta - \sum_{n=0}^{k} \frac{m_n}{M_k}\, F_2\left(\frac{\zeta t}{t - t_n}\right) + \frac{1}{t} \sum_{n=0}^{k} \frac{m_n\, t_n}{M_k}\, F_2\left(\frac{\zeta t}{t - t_n}\right) = \frac{\kappa_k}{t}$$

42

or, finally,

$$t = \frac{\kappa_k - \sum_{n=0}^{k} \frac{m_n t_n}{M_k} F_2\left(\frac{\zeta t}{t - t_n}\right)}{\nu_k + \sigma_k \zeta - \sum_{n=0}^{k} \frac{m_n}{M_k} F_2\left(\frac{\zeta t}{t - t_n}\right)} \qquad t_{ak} \le t < t_{a(k+1)}. \qquad (4.17)$$

(This solution recovers the two-pulse solution derived previously when $k = 1$.) All $[t, \zeta(t)]$ pairs that lie on the foil trajectory will satisfy this implicit equation. Such solutions will, in general, have to be found numerically, one regime at a time.

As usual, κ_k is determined by the condition that the regimes must meet continuously at $t = t_{ak}$. Using $\zeta_{ak} \equiv \zeta(t_{ak})$ this boundary condition is

$$t_{ak} = \frac{\kappa_k - \sum_{n=0}^{k} \frac{m_n t_n}{M_k} F_2\left(\frac{\zeta_{ak} t_{ak}}{t_{ak} - t_n}\right)}{\nu_k + \sigma_k \zeta_{ak} - \sum_{n=0}^{k} \frac{m_n}{M_k} F_2\left(\frac{\zeta_{ak} t_{ak}}{t_{ak} - t_n}\right)}$$

so

$$\kappa_k = t_{ak} \left[\nu_k + \sigma_k \zeta_{ak} - \sum_{n=0}^{k} \frac{m_n}{M_k} F_2\left(\frac{\zeta_{ak} t_{ak}}{t_{ak} - t_n}\right)\right] + \sum_{n=0}^{k} \frac{m_n t_n}{M_k} F_2\left(\frac{\zeta_{ak} t_{ak}}{t_{ak} - t_n}\right). \qquad (4.18)$$

(This is likewise consistent with the two-pulse solution when $k = 1$.)

43

References

[1] Tregillis, I. L. and Koskelo, Aaron. "Analytic Solutions as a Tool for Verification and Validation of a Multiphysics Model," *J. Verif. Valid. Uncert.* **4**(4):041004 (2019)

[2] Tregillis, I. L. "(U) An Analytic Study of Piezoelectric Ejecta Mass Measurements," Technical Report LA-UR-17-21218, Los Alamos National Laboratory, Los Alamos, NM (2017)

[3] Tregillis, I. L. "(U) Boundary Conditions for Ejecta Source Models with Stationary Velocity Distributions," Technical Report LA-UR-18-27420, Los Alamos National Laboratory, Los Alamos, NM (2018)

[4] Asay, J. R., Mix, L. P., and Perry, F. C. "Ejection of material from shocked surfaces," *Appl. Phys. Lett.* **29**:284 (1976)

[5] Asay, J. R. "Thick-plate technique for measuring ejecta from shocked surfaces," *J. Appl. Phys.* **49**:6173 (1978)

[6] Steele, P. T., Jacoby, B. A., Compton, S. M., and Sinibaldi, J. O. "Advancements in Ejecta Diagnostics at LLNL," *J. Dyn. Beh. Mat.* **3**:253 (2017)

[7] Vogan, W. S., Anderson, W. W., Grover, M., Hammerberg, J. E., King, N. S. P., Lamoreaux, S. K., Macrum, G., Morley, K. B., Rigg, P. A., Stevens, G. D., Turley, W. D., Veeser, L. R., and Buttler, W. T. "Piezoelectric characterization of ejecta from shocked tin surfaces," *J. Appl. Phys.* **98**:113508 (2005)

[8] Hammerberg, James E., Harrison, Alan K., Williams, Matthew W., Margolin, Len, G., and Francois, M. M. "(U) A Self-Similarity Velocity Distribtion (SSVD) Source Model for Ejecta: Theory, Implementation and Verification," Technical Report LA-CP-17-00235, Los Alamos National Laboratory, Los Alamos, NM (2017)

[9] Hammerberg, J. E., Buttler, W. T., Llobet, A., Morris, C., Goett, J., Manzanares, R., Saunders, A., Schmidt, D., Tainter, A., Vogan-McNeil, W., and Wilde, C. "Proton Radiography Measurements and Models of Ejecta Structure in Shocked Sn," *AIP Conf. Proc.* **1979**:080006 (2018).

[10] Buttler, W. T., Oró, D. M., Olson, R. T., Cherne, F. J., Hammerberg, J. E., Hixson, R. S., Monfared, S. K., Pack, C. L., Rigg, P. A., Stone, J. B., and Terrones, G. "Second shock ejecta measurements with an explosively driven two-shockwave drive," *J. Appl. Phys.* **116**:103519 (2014)